

Guillermo Durand  Laboratoire de Mathématiques d'Orsay, Université Paris-Saclay

Date published: 2025-01-31 Last modified: 2025-01-31

Abstract

This paper presents a new algorithm (and an additional trick) that allows to compute fastly an entire curve of post hoc bounds for the False Discovery Proportion when the underlying bound $V_{\mathfrak{R}}^*$ construction is based on a reference family \mathfrak{R} with a forest structure à la [Durand et al. \(2020\)](#). By an entire curve, we mean the values $V_{\mathfrak{R}}^*(S_1), \dots, V_{\mathfrak{R}}^*(S_m)$ computed on a path of increasing selection sets $S_1 \subsetneq \dots \subsetneq S_m$, $|S_t| = t$. The new algorithm leverages the fact that going from S_t to S_{t+1} is done by adding only one hypothesis.

Keywords: multiple testing, algorithmic, post hoc inference, false discovery proportion, confidence bound

1 Contents

2	1 Introduction	2
3	2 Notation and reference family methodology	3
4	2.1 Multiple testing notation	3
5	2.2 Post hoc bounds with reference families	3
6	2.3 Regions with a forest structure	4
7	3 New algorithms	7
8	3.1 Pruning the forest	7
9	3.2 Fast algorithm to compute a curve of confidence bounds on a path of selection sets	9
10	3.3 Illustration on a detailed example	11
11	3.4 Proof of Theorem 3.1	17
12	3.4.1 Derivation of (18)	17
13	3.4.2 Proof of (16) and (17)	17
14	4 Implementation	23
15	5 Numerical experiments	24
16	6 Conclusion	27
17	7 Acknowledgements	27
18	References	27
19	Session information	29

¹Corresponding author: guillermo.durand@universite-paris-saclay.fr

20 **1 Introduction**

21 Multiple testing theory is often used for exploratory analysis, like Genome-Wide Association Studies,
 22 where multiple features are tested to find promising ones. Classical multiple testing theory like
 23 Family-Wise Error Rate (FWER) control or False Discovery Rate (FDR) control (Benjamini and
 24 Hochberg, 1995) can be used, but a more recent trend consists in the computation of post hoc bounds,
 25 also named post selection bounds or confidence envelopes, for the number of false positives, or,
 26 equivalently, for the False Discovery Proportion (FDP). This approach is notably advocated for in the
 27 context of exploratory research by (Goeman and Solari, 2011, Section 1).

28 Mathematically speaking, a confidence upper bound (we prefer to say upper bound instead of envelope
 29 for obvious reasons) is a function $\hat{V} : \mathcal{P}(\mathbb{N}_m^*) \rightarrow \mathbb{N}_m$, where $\mathbb{N}_m = \{0, \dots, m\}$, $\mathbb{N}_m^* = \{1, \dots, m\}$ and m
 30 is the number of hypotheses, such that

$$\forall \alpha \in]0, 1[, \mathbb{P}(\forall S \subseteq \mathbb{N}_m^*, |S \cap \mathcal{H}_0| \leq \hat{V}(S)) \geq 1 - \alpha. \quad (1)$$

31 Here, α is a target error rate and \mathcal{H}_0 is the set of hypotheses indices that are true null hypotheses.
 32 Note that the construction of \hat{V} depends on α and on the random data X and the dependence is omitted
 33 to lighten notation and because there is no ambiguity. The meaning of Equation (1) is that \hat{V} provides
 34 an upper bound of the number of null hypotheses in S for any selection set $S \subseteq \mathbb{N}_m^*$, which allows
 35 the user to perform post hoc selection on their data without breaching the statistical guarantee. Also
 36 note that by dividing by $|S| \vee 1$ in Equation (1) we also get a confidence bound for the FDP:

$$\forall \alpha \in]0, 1[, \mathbb{P}\left(\forall S \subseteq \mathbb{N}_m^*, \text{FDP}(S) \leq \frac{\hat{V}(S)}{|S| \vee 1}\right) \geq 1 - \alpha. \quad (2)$$

37 So post hoc bounds provide ways to construct FDP-controlling sets instead of FDR-controlling sets,
 38 which is much more desirable given the nature of the FDR as an expected value. See for example
 39 (Bogdan et al., 2015, Figure 4) for a credible example where the FDR is controlled but the FDP has a
 40 highly undesirable behavior (either 0 because no discoveries at all are made, either higher than the
 41 target level).

42 The first confidence bounds are found in Genovese and Wasserman (2006) and Meinshausen (2006),
 43 although, in the latter, only for selection sets of the form $\{i \in \mathbb{N}_m : P_i \leq t\}$ where P_i is the p -value
 44 associated to the null hypothesis $H_{0,i}$. In Goeman and Solari (2011) the authors re-wrote the generic
 45 construction of Genovese and Wasserman (2006) in terms of closed testing Marcus et al. (1976),
 46 proposed several practical constructions and sparked a new interest in multiple testing procedures
 47 based on confidence envelopes. This work was followed by a prolific series of works like Meijer et al.
 48 (2015) or Vesely et al. (2023). In Blanchard et al. (2020), the authors introduce the new point of view
 49 of references families (see Section 2.2) to construct post hoc bounds, and show the links between this
 50 meta-technique and the closed testing one, along with new bounds.

51 Following the reference family trail, in Durand et al. (2020) the authors introduce new reference
 52 families with a special set-theoretic constraint that allows an efficient computation of the bound
 53 denoted by $V_{\mathfrak{R}}^*$ on a single selection set S . The problem is that one often wants to compute $V_{\mathfrak{R}}^*$ on a
 54 whole path of selection sets $(S_t)_{t \in \mathbb{N}_m^*}$, for example the hypotheses attached to the t smallest p -values.
 55 Whereas the algorithm provided in the aforementioned work (Durand et al., 2020, Algorithm 1),
 56 which is reproduced here, see Algorithm 1, is fast for a single evaluation, it is slow and inefficient
 57 to repeatedly call it to compute each $V_{\mathfrak{R}}^*(S_t)$. If the S_t 's are nested, and growing by one, that is
 58 $S_1 \subsetneq \dots \subsetneq S_m$ and $|S_t| = t$, there is a way to efficiently compute $(V_{\mathfrak{R}}^*(S_t))_{t \in \mathbb{N}_m}$ by leveraging the nested
 59 structure.

60 This is the main contribution of the present paper: a new and fast algorithm computing the curve
 61 $(V_{\mathfrak{R}}^*(S_t))_{t \in \mathbb{N}_m}$ for a nested path of selection sets, that is presented in Section 3.2. An additional

62 algorithm that can speed up computations both for the single-evaluation algorithm and the new
 63 curve-evaluation algorithm is also presented, in Section 3.1. A detailed example illustrating how
 64 the new algorithms work is provided in Section 3.3, and the proof that the fast algorithm indeed
 65 computes correctly the curve is in Section 3.4. In Section 2.1, all necessary notation and vocabulary is
 66 re-introduced, most of it being the same as in Durand et al. (2020). In Section 4 we discuss the current
 67 implementations of all the presented algorithms in the R (R Core Team, 2024) package `sanssouci`
 68 (Neuvial et al., 2024). Finally, a few numerical experiments are presented in Section 5 to
 69 demonstrate the computation time gain.

70 2 Notation and reference family methodology

71 2.1 Multiple testing notation

72 As is usual in multiple testing theory, we consider a probability space $(\Omega, \mathcal{A}, \mathbb{P})$, a model \mathcal{P} on a
 73 measurable space $(\mathcal{X}, \mathfrak{X})$, and data that is represented by a random variable $X : (\Omega, \mathcal{A}) \rightarrow (\mathcal{X}, \mathfrak{X})$
 74 with $X \sim P \in \mathcal{P}$, that is, the law of X is comprised in the model \mathcal{P} .

75 Then we consider $m \geq 1$ null hypotheses $H_{0,1}, \dots, H_{0,m}$ which formally are submodels, that is subsets
 76 of \mathcal{P} . The associated alternative hypotheses $H_{1,1}, \dots, H_{1,m}$ are submodels such that $H_{0,i} \cap H_{1,i} = \emptyset$
 77 for all $i \in \mathbb{N}_m^*$. We denote by $\mathcal{H}_0 = \mathcal{H}_0(P)$ (the dependence in P will be dropped when there is no
 78 ambiguity) the set of all null hypotheses that are true, that is $\mathcal{H}_0(P) = \{i \in \mathbb{N}_m^* : P \in H_{0,i}\}$. In
 79 other words, $H_{0,i}$ is true if and only if $i \in \mathcal{H}_0$. For testing each $H_{0,i}, i \in \mathbb{N}_m^*$, we have at hand a
 80 p -value $p_i = p_i(X)$ (the dependence in X will be dropped when there is no ambiguity) which is a
 81 random variable with the following property : if $i \in \mathcal{H}_0$, then the law of p_i is super-uniform, which
 82 is sometimes denoted $\mathcal{L}(p_i) \succeq \mathcal{U}([0, 1])$. This means that in such case, the cumulative distribution
 83 function (cdf) of p_i is always smaller than or equal to the cdf of a random variable $U \sim \mathcal{U}([0, 1])$:

$$\forall x \in \mathbb{R}, \mathbb{P}(p_i \leq x) \leq \mathbb{P}(U \leq x) = 0 \vee (x \wedge 1). \quad (3)$$

84 For every subset of hypotheses $S \subseteq \mathbb{N}_m^*$, let $V(S) = |S \cap \mathcal{H}_0|$. If we think of S as a selection set of
 85 hypotheses deemed significant, $V(S)$ is then the number of false positives (FP) in S . $V(S)$ is our main
 86 object of interest and the quantity that we wish to over-estimate with confidence upper bounds (see
 87 Equation (1) or the more formal Equation (4) below).

88 Finally let us consider the following toy example, that will be re-used in the remainder of the paper.

89 **Example 2.1** (Gaussian one-sided). In this case we assume that $X = (X_1, \dots, X_m)$ is a Gaussian
 90 vector and the null hypotheses refer to the nullity of the means in contrast to their positivity. That
 91 is, formally, $(\mathcal{X}, \mathfrak{X}) = (\mathbb{R}^m, \mathcal{B}(\mathbb{R}^m))$, $\mathcal{P} = \{\mathcal{N}(\boldsymbol{\mu}, \Sigma) : \forall j \in \mathbb{N}_m^*, \mu_j \geq 0, \Sigma \text{ positive semidefinite}\}$, for
 92 each $i \in \mathbb{N}_m^*$, $H_{0,i} = \{\mathcal{N}(\boldsymbol{\mu}, \Sigma) \in \mathcal{P} : \mu_i = 0\}$ and $H_{1,i} = \{\mathcal{N}(\boldsymbol{\mu}, \Sigma) \in \mathcal{P} : \mu_i > 0\}$. Then we can
 93 construct p -values by letting $p_i(X) = \bar{\Phi}(X_i) = 1 - \Phi(X_i)$, where Φ denotes the cdf of $\mathcal{N}(0, 1)$ and $\bar{\Phi}$
 94 the associated survival function.

95 2.2 Post hoc bounds with reference families

96 With the formalism introduced in last section, a confidence upper bound is a functional $\hat{V} : \mathcal{X} \times]0, 1[\rightarrow$
 97 $(\mathcal{P}(\mathbb{N}_m^*) \rightarrow \mathbb{N}_m)$ such that,

$$\forall P \in \mathcal{P}, \forall X \sim P, \forall \alpha \in]0, 1[, \mathbb{P}(\forall S \subseteq \mathbb{N}_m^*, V(S) \leq \hat{V}(X, \alpha)(S)) \geq 1 - \alpha. \quad (4)$$

98 In the remainder, the dependence in (X, α) will be dropped when there is no ambiguity and $\hat{V}(X, \alpha)$
 99 will simply be written \hat{V} .

100 As said in the Introduction, many constructions, ultimately theoretically equivalent but differing by
 101 the practical steps involved, exist, and in this paper we focus on the meta-construction of [Blanchard
 et al. \(2020\)](#) based on reference families. A reference family is a family $\mathfrak{R} = \mathfrak{R}(X, \alpha) = (R_k, \zeta_k)_{k \in \mathcal{K}}$
 102 with $|\mathcal{K}| \leq 2^m$, $R_k \subseteq \mathbb{N}_m^*$, $\zeta_k \in \{0, \dots, |R_k|\}$ where everything (that is, \mathcal{K} and all the R_k and ζ_k) depends
 103 on (X, α) but the dependency is not explicitly written. The R_k are all distinct. We also define the
 104 following error criterion for a reference family, named Joint Error Rate (JER):
 105

$$\text{JER}(\mathfrak{R}) = \mathbb{P}(\exists k \in \mathcal{K}, |R_k \cap \mathcal{H}_0| > \zeta_k) = \mathbb{P}(\exists k \in \mathcal{K}, V(R_k) > \zeta_k). \quad (5)$$

106 In the following, we are only interested in reference families that control the JER at level α :

$$\forall P \in \mathcal{P}, \forall X \sim P, \forall \alpha \in]0, 1[, 1 - \text{JER}(\mathfrak{R}(X, \alpha)) = \mathbb{P}(\forall k \in \mathcal{K}, V(R_k) \leq \zeta_k) \geq 1 - \alpha. \quad (6)$$

107 Note that Equation (6) is really similar to Equation (4) except that the uniform guarantee, instead of
 108 being over all $S \subseteq \mathbb{N}_m^*$, is only over all the $R_k \subseteq \mathbb{N}_m^*$, $k \in \mathcal{K}$, with \mathcal{K} having cardinality potentially
 109 much smaller than 2^m . A global confidence bound is then derived from a JER-controlling reference
 110 family by interpolation. Let

$$\mathcal{A}(\mathfrak{R}) = \{A \subseteq \mathbb{N}_m^* : \forall k \in \mathcal{K}, |R_k \cap A| \leq \zeta_k\}. \quad (7)$$

111 What says the JER control is that $\mathcal{H}_0 \in \mathcal{A}(\mathfrak{R})$. We leverage this information with the following
 112 confidence bound construction:

$$V_{\mathfrak{R}}^*(S) = \max_{A \in \mathcal{A}(\mathfrak{R})} |S \cap A| \quad (8)$$

113 which optimally uses the information provided by the JER control of the reference family, as proven
 114 by Proposition 2.1 of [Blanchard et al. \(2020\)](#). Because of the $\max_{A \in \mathcal{A}(\mathfrak{R})}$, the computation of $V_{\mathfrak{R}}^*(S)$
 115 is generally intractable (see Proposition 2.2 of [Blanchard et al. \(2020\)](#)), but for specific structures of
 116 reference families, a polynomial computation can be derived. This is the topic of [Durand et al. \(2020\)](#)
 117 and of next section.

118 2.3 Regions with a forest structure

119 The core concept of this section is to assume that the regions R_k 's of the reference family are what
 120 we called in [Durand et al. \(2020\)](#) a forest structure, that is two regions are either disjoint or nested:

$$\forall k, k' \in \mathcal{K}, R_k \cap R_{k'} \in \{R_k, R_{k'}, \emptyset\}. \quad (9)$$

121 Representing the R_k 's with a directed graph, where there is an oriented edge $R_k \leftarrow R_{k'}$ if and only if
 122 $R_k \subset R_{k'}$ and there is no $R_{k''}$ such that $R_k \subsetneq R_{k''} \subsetneq R_{k'}$ gives a forest, hence the name. See Example 2.2
 123 and its representation in Figure 1.

124 We also need to introduce the notion of depth with the following function:

$$\phi : \begin{cases} \mathcal{K} & \rightarrow \mathbb{N}^* \\ k & \mapsto 1 + |\{k' \in \mathcal{K} : R_k \subsetneq R_{k'}\}|. \end{cases} \quad (10)$$

125 **Example 2.2.** Let $m = 25$, $R_1 = \{1, \dots, 20\}$, $R_2 = \{1, 2\}$, $R_3 = \{3, \dots, 10\}$, $R_4 = \{11, \dots, 20\}$, $R_5 =$
 126 $\{5, \dots, 10\}$, $R_6 = \{11, \dots, 16\}$, $R_7 = \{17, \dots, 20\}$, $R_8 = \{21, 22\}$, $R_9 = \{22\}$. This is the same example as
 127 Example 2 of [Durand et al. \(2020\)](#) and it is graphically depicted in Figure 1. The sets R_1, R_8 are of
 128 depth 1; the sets R_2, R_3, R_4, R_9 are of depth 2; the sets R_5, R_6, R_7 are of depth 3.

129 Another tool of [Durand et al. \(2020\)](#) that will be used is its Lemma 2, that is the identification
 130 of \mathfrak{R} with a set $\mathcal{C} \subset \{(i, j) \in (\mathbb{N}_N^*)^2 : i \leq j\}$ such that for $(i, j), (i', j') \in \mathcal{C}$, $\{i, \dots, j\} \cap \{i', \dots, j'\} \in$

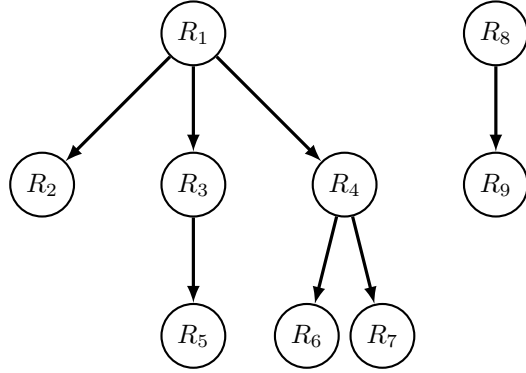


Figure 1: The regions of Example 2.2.

131 $\{\emptyset, \{i, \dots, j\}, \{i', \dots, j'\}\}$. With this identification, each $R_k = R_{(i,j)}$ can be written as $P_{i:j} = \bigcup_{i \leq n \leq j} P_n$
 132 where $(P_n)_{1 \leq n \leq N}$ is a partition of \mathbb{N}_m^* . The P_n 's were called atoms in Durand et al. (2020) because
 133 they have the thinnest granularity in the structure, but to continue the analogy with graphs, forests
 134 and trees, they can also be called leafs. See Example 2.3 for a concrete example.

135 **Example 2.3** (Continuation of Example 2.2). For the reference family given in Example 2.2, a partition
 136 of atoms is given by $P_1 = R_2$, $P_2 = R_3 \setminus R_5$, $P_3 = R_5$, $P_4 = R_6$, $P_5 = R_7$, $P_6 = R_8 \setminus R_9$, $P_7 = R_9$,
 137 $P_8 = \mathbb{N}_m^* \setminus \{R_1 \cup R_8\}$. Then $R_1 = P_{1:5}$, $R_3 = P_{2:3}$, $R_4 = P_{4:5}$ and $R_8 = P_{6:7}$. Note that not all atoms
 138 are regions of the family. Those new labels are graphically depicted in Figure 2. The nodes that
 139 correspond to atoms that are not in the family are depicted with a dashed circle, and all atoms are
 140 depicted in gray. This is the same example as Example 3 of Durand et al. (2020).

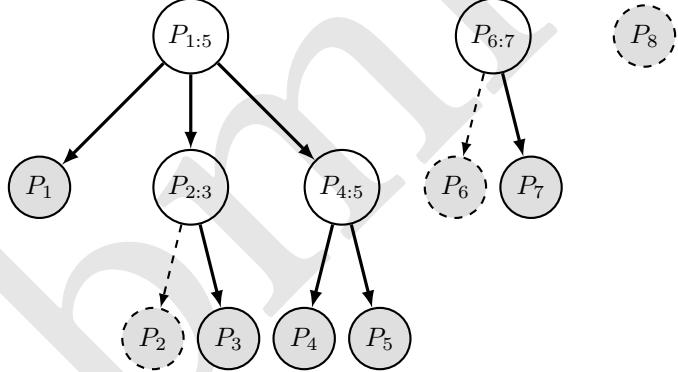


Figure 2: The regions of Example 2.2 but with the labels of Example 2.3.

141 When all leaves are regions of the family, it is said that the family is complete. If this is not the
 142 case, the family can easily be completed by adding the missing leaves (and using their cardinality as
 143 associated ζ) without changing the value $V_{\mathfrak{R}}^*$. See Definition 2, Lemma 6 and Algorithm 2 of Durand
 144 et al. (2020) for the details.

145 Durand et al. (2020) also proved in their Theorem 1 that:

$$V_{\mathfrak{R}}^*(S) = \min_{Q \subseteq \mathfrak{R}} \left(\sum_{k' \in Q} \zeta_{k'} \wedge |S \cap R_{k'}| + \left| S \setminus \bigcup_{k' \in Q} R_{k'} \right| \right) \quad (11)$$

146 and, even better, in their Corollary 1 (iii) that:

$$V_{\mathfrak{R}}^*(S) = \min_{Q \in \mathfrak{P}} \sum_{k' \in Q} \zeta_{k'} \wedge |S \cap R_{k'}|, \quad (12)$$

147 provided that the family is complete. Here, $\mathfrak{P} \subseteq \mathcal{P}(\mathcal{K})$ is the set of subsets of \mathcal{K} that realize a
 148 partition, that is, the set of $Q \subseteq \mathcal{K}$ such that the $R_k, k \in Q$, form a partition of \mathbb{N}_m^* . So the minimum
 149 in Equation (12) is over way less elements than in Equation (11).

150 Finally, that paper provides a polynomial algorithm to $V_{\mathfrak{R}}^*(S)$ for a single $S \subseteq \mathbb{N}_m^*$, which we reproduce
 151 here in Algorithm 1. The family is assumed complete, otherwise the first step would be to complete
 152 it. In the original paper, \mathcal{K}^h used to designate the elements of \mathcal{K} at depth h plus the atoms at depth
 153 $\leq h$. Actually one can realize that the last assumption is not needed for this algorithm to perform
 154 exactly the same, with the added benefit of not repeating computations at the atoms that don't have
 155 the maximal depth. The only change is that sometimes $Succ_k$ can be empty, in which case we simply
 156 let $newVec_k = \zeta_k \wedge |S \cap R_k|$. Thus, here in this paper, we define \mathcal{K}^h as only the elements of \mathcal{K} at
 157 depth h (the previous intricate definition may still be necessary for the proof of Theorem 1 of Durand
 158 et al. (2020)): $\mathcal{K}^h = \{(i, j) \in \mathcal{K} : \phi(i, j) = h\}, h \geq 1$. This is the only deviation from the notation of
 159 Durand et al. (2020). Finally note that in the ongoing analogy with graph theory, the elements of \mathcal{K}^1
 160 are the roots of the different trees making up the forest.

Algorithm 1 Computation of a given $V_{\mathfrak{R}}^*(S)$

```

1: procedure VSTAR( $S, \mathfrak{R} = (R_k, \zeta_k)_{k \in \mathcal{K}}$  with  $\mathfrak{R}$  complete)
2:    $H \leftarrow \max_{k \in \mathcal{K}} \phi(k)$  ▷ maximum depth
3:   for  $h = H - 1, \dots, 1$  do
4:      $\mathcal{K}^h \leftarrow \{k \in \mathcal{K} : \phi(k) = h\}$ 
5:      $newVec \leftarrow (0)_{k \in \mathcal{K}^h}$ 
6:     for  $k \in \mathcal{K}^h$  do
7:        $Succ_k \leftarrow \{k' \in \mathcal{K}^{h+1} : R_{k'} \subseteq R_k\}$ 
8:       if  $Succ_k = \emptyset$  then
9:          $newVec_k \leftarrow \zeta_k \wedge |S \cap R_k|$ 
10:      else
11:         $newVec_k \leftarrow \min(\zeta_k \wedge |S \cap R_k|, \sum_{k' \in Succ_k} Vec_{k'})$ 
12:      end if
13:    end for
14:     $Vec \leftarrow newVec$ 
15:  end for
16:  return  $\sum_{k \in \mathcal{K}^1} Vec_k$ 
17: end procedure

```

💡 Tip

In the practical implementation of this algorithm (and of the following Algorithm 2), Vec and $newVec$ are always of size N (the number of leaves) instead of the cardinality of \mathcal{K}^h . And the sum $\sum_{k' \in Succ_k} Vec_{k'}$ is really easy to compute: if $R_k = R_{(i_0, i_p-1)} = \bigcup_{j=1}^p R_{(i_{j-1}, i_j-1)} = \bigcup_{i_0 \leq n \leq i_p-1} P_n \in \mathcal{K}^h$ for some $p \geq 2$, a strictly increasing sequence (i_0, \dots, i_p) and $R_{(i_{j-1}, i_j-1)} \in \mathcal{K}^{h+1}$ for all $1 \leq j \leq p$, then we simply sum Vec over the indices from i_0 to $i_p - 1$. After that, the computed quantity is set in $newVec$ at index i_0 . So actually computing $Succ_k$ is not needed and not done.

161
 162 The computation time of the algorithm is in $O(m|\mathcal{K}|)$, which is fast for a single evaluation, but calling
 163 it repeatedly on a path of selection sets $(S_t)_{t \in \mathbb{N}_m^*}$ has complexity $O(m^2|\mathcal{K}|)$ which is not desirable and
 164 makes computations difficult in practice, hence the need for a new, faster algorithm.

165 *Remark 2.1.* The specific computation of the R_k 's and the ζ_k 's such that Equation (6) holds is outside
 166 the scope of the present paper, but different constructions can be found in Blanchard et al. (2020),

¹⁶⁷ Durand et al. (2020) or Blain et al. (2022) for example.

¹⁶⁸ 3 New algorithms

¹⁶⁹ 3.1 Pruning the forest

¹⁷⁰ We remark the simple fact that if, for example, $(1, 1), (2, 2), (1, 2) \in \mathcal{K}$, and $\zeta_{(1,2)} \geq \zeta_{(1,1)} + \zeta_{(2,2)}$, then
¹⁷¹ $R_{(1,2)}$ never contributes to the computation of any $V_{\mathfrak{R}}^*(S)$ and it could just be removed from \mathfrak{R} . We
¹⁷² now formalize and prove this pruning scheme.

¹⁷³ **Definition 3.1** (Pruning). We define by \mathcal{K}^{pr} (\mathcal{K} pruned) the set of elements of \mathcal{K} such that we
¹⁷⁴ removed all (i, i') such that there exists $p \geq 2$ and integers i_1, \dots, i_{p-1} such that, when setting $i_0 = i$
¹⁷⁵ and $i_p = i' + 1$, the sequence (i_0, \dots, i_p) is strictly increasing, $(i_{j-1}, i_j - 1) \in \mathcal{K}$ for all $1 \leq j \leq p$ and
¹⁷⁶ finally $\zeta_{(i,i')} = \zeta_{(i_0, i_p - 1)} \geq \sum_{j=1}^p \zeta_{(i_{j-1}, i_j - 1)}$.

¹⁷⁷ An important note is that for a removed $(i, i') \in \mathcal{K} \setminus \mathcal{K}^{\text{pr}}$, we can always choose the indices i_1, \dots, i_{p-1}
¹⁷⁸ such that actually $(i_j, i_{j+1} - 1) \in \mathcal{K}^{\text{pr}}$ and not only \mathcal{K} , because if $(i_j, i_{j+1} - 1) \in \mathcal{K} \setminus \mathcal{K}^{\text{pr}}$ it can itself
¹⁷⁹ be fragmented, and this decreasing recursion eventually ends (the later possible being at the atoms
¹⁸⁰ of the forest structure). Also note that removing elements from \mathcal{K} does not alter the fact that we
¹⁸¹ have at hand a forest structure, that is, the reference family defined by $\mathfrak{R}^{\text{pr}} = (R_k, \zeta_k)_{k \in \mathcal{K}^{\text{pr}}}$ has a
¹⁸² forest structure. Because pruning a forest structure does not touch the atoms, note finally that if \mathcal{K}
¹⁸³ is complete then so is \mathcal{K}^{pr} .

¹⁸⁴ The following proposition states that pruning the forest does not alter the bound.

¹⁸⁵ **Proposition 3.1.** *For any $S \subseteq \mathbb{N}_m^*$, $V_{\mathfrak{R}}^*(S) = V_{\mathfrak{R}^{\text{pr}}}^*(S)$.*

¹⁸⁶ *Proof.* Recall Equation (11) and, because \mathfrak{R}^{pr} also has a forest structure,

$$V_{\mathfrak{R}^{\text{pr}}}(S) = \min_{Q \subseteq \mathcal{K}^{\text{pr}}} \left(\sum_{k' \in Q} \zeta_{k'} \wedge |S \cap R_{k'}| + \left| S \setminus \bigcup_{k' \in Q} R_{k'} \right| \right), \quad (13)$$

¹⁸⁷ so we immediately get that $V_{\mathfrak{R}}^*(S) \leq V_{\mathfrak{R}^{\text{pr}}}^*(S)$.

¹⁸⁸ Let any $Q \subseteq \mathcal{K}$. We split Q in A elements of $\mathcal{K} \setminus \mathcal{K}^{\text{pr}}$, denoted $(i_{0,a}, i_{p_a, a} - 1)$, $1 \leq a \leq A$ for some $p_a \geq 2$,
¹⁸⁹ and B elements of \mathcal{K}^{pr} , simply denoted k_b , $1 \leq b \leq B$. By the definition of \mathcal{K}^{pr} and the previous
¹⁹⁰ remarks, for any $1 \leq a \leq A$, there exist integers $i_{1,a}, \dots, i_{p_a-1, a}$ such that $i_{0,a} < i_{1,a} < \dots < i_{p_a-1, a} < i_{p_a, a}$,
¹⁹¹ $(i_{j-1, a}, i_{j, a} - 1) \in \mathcal{K}^{\text{pr}}$ for all $1 \leq j \leq p_a$, and $\zeta_{(i_{0,a}, i_{p_a, a} - 1)} \geq \sum_{j=1}^{p_a} \zeta_{(i_{j-1, a}, i_{j, a} - 1)}$. Now let

$$Q^{\text{pr}} = \{k_b : 1 \leq b \leq B\} \cup \{(i_{j-1, a}, i_{j, a} - 1) : 1 \leq a \leq A, 1 \leq j \leq p_a\}. \quad (14)$$

¹⁹² We have that $Q^{\text{pr}} \subseteq \mathcal{K}^{\text{pr}}$ and $\bigcup_{k \in Q} R_k = \bigcup_{k \in Q^{\text{pr}}} R_k$. Then,

$$\begin{aligned} \sum_{k \in Q} \zeta_k \wedge |S \cap R_k| + \left| S \setminus \bigcup_{k \in Q} R_k \right| &= \sum_{b=1}^B \zeta_{k_b} \wedge |S \cap R_{k_b}| \\ &\quad + \sum_{a=1}^A \zeta_{(i_{0,a}, i_{p_a, a} - 1)} \wedge |S \cap R_{(i_{0,a}, i_{p_a, a} - 1)}| \\ &\quad + \left| S \setminus \bigcup_{k \in Q} R_k \right|, \end{aligned}$$

193 but for all $1 \leq a \leq A$,

$$\begin{aligned}\zeta_{(i_{0,a}, i_{p_a,a}-1)} &\geq \sum_{j=1}^{p_a} \zeta_{(i_{j-1,a}, i_{j,a}-1)} \\ &\geq \sum_{j=1}^{p_a} \zeta_{(i_{j-1,a}, i_{j,a}-1)} \wedge |S \cap R_{(i_{j-1,a}, i_{j,a}-1)}|,\end{aligned}$$

194 so the term $\sum_{a=1}^A \zeta_{(i_{0,a}, i_{p_a,a}-1)} \wedge |S \cap R_{(i_{0,a}, i_{p_a,a}-1)}|$ is greater than or equal to

$$\sum_{a=1}^A \left(\sum_{j=1}^{p_a} \zeta_{(i_{j-1,a}, i_{j,a}-1)} \wedge |S \cap R_{(i_{j-1,a}, i_{j,a}-1)}| \right) \wedge |S \cap R_{(i_{0,a}, i_{p_a,a}-1)}|,$$

195 which is simply equal to

$$\sum_{a=1}^A \sum_{j=1}^{p_a} \zeta_{(i_{j-1,a}, i_{j,a}-1)} \wedge |S \cap R_{(i_{j-1,a}, i_{j,a}-1)}|.$$

196 Furthermore $|S \setminus \bigcup_{k \in Q} R_k| = |S \setminus \bigcup_{k \in Q^{\text{pr}}} R_k|$ so finally:

$$\begin{aligned}\sum_{k \in Q} \zeta_k \wedge |S \cap R_k| + \left| S \setminus \bigcup_{k \in Q} R_k \right| &\geq \sum_{k \in Q^{\text{pr}}} \zeta_k \wedge |S \cap R_k| + \left| S \setminus \bigcup_{k \in Q^{\text{pr}}} R_k \right| \\ &\geq V_{\mathcal{R}^{\text{pr}}}^*(S).\end{aligned}\tag{15}$$

197 Note that Equation (15) is true even if there are some $b \in \{1, \dots, B\}$, $a \in \{1, \dots, A\}$, $j \in \{1, \dots, p_a\}$ such
198 that $k_b = (i_{j-1,a}, i_{j,a}-1)$. We minimize over all Q to get that $V_{\mathcal{R}}^*(S) \geq V_{\mathcal{R}^{\text{pr}}}^*(S)$. \square \square

199 This gives a practical way to speed up computations by first pruning the family before computing
200 any $V_{\mathcal{R}}^*(S)$, because \mathcal{K}^{pr} is smaller than \mathcal{K} , and by the above Proposition there is no theoretical loss
201 in doing so.

202 Furthermore, pruning can be done really simply by following Algorithm 1 for $S = \mathbb{N}_m^*$, and pruning
203 when appropriate. This gives the following Algorithm 2, assuming, for simplicity, that the family is
204 complete. The computation time of the algorithm is the same as Algorithm 1, that is $O(m|\mathcal{K}|)$. Note
205 that the only differences between Algorithm 2 and Algorithm 1 are the pruning step and ζ_k replacing
206 $\zeta_k \wedge |S \cap R_k|$, because $\zeta_k \leq |R_k|$ and here $S = \mathbb{N}_m^*$, so $\zeta_k \wedge |\mathbb{N}_m^* \cap R_k| = \zeta_k$. Also note that the algorithm
207 returns $V_{\mathcal{R}}^*(\mathbb{N}_m^*)$ as a by-product. The following proposition states that Algorithm 2 indeed produces
208 the pruned region as in Definition 3.1.

209 **Proposition 3.2.** *The final \mathcal{L} returned by Algorithm 2 is equal to \mathcal{K}^{pr} : $\mathcal{L} = \mathcal{K}^{\text{pr}}$.*

210 *Proof.* First, $\mathcal{K} \setminus \mathcal{L} \subseteq \mathcal{K} \setminus \mathcal{K}^{\text{pr}}$ is trivial: a k such that $\zeta_k \geq \sum_{k' \in \text{Succ}_k} \text{Vec}_{k'}$ obviously satisfies the
211 condition of Definition 3.1 to be pruned.

212 Now let $(i, i') \in \mathcal{K} \setminus \mathcal{K}^{\text{pr}}$ an element that is pruned by Definition 3.1, so there exists $p \geq 2$
213 and integers i_1, \dots, i_{p-1} such that, when setting $i_0 = i$ and $i_p = i' + 1$, the sequence (i_0, \dots, i_p) is
214 strictly increasing, $(i_{j-1}, i_j - 1) \in \mathcal{K}$ for all $1 \leq j \leq p$ and finally $\zeta_{(i, i')} = \zeta_{(i_0, i_p - 1)} \geq \sum_{j=1}^p \zeta_{(i_{j-1}, i_j - 1)}$.
215 Then by the proof of Theorem 1 of Durand et al. (2020) but applied to $S = R_{(i, i')}$ we have that
216 $\sum_{j=1}^p \zeta_{(i_{j-1}, i_j - 1)} \geq \sum_{k' \in \text{Succ}_{(i, i')}} \text{Vec}_{k'}$ (see the unnumbered line just above Equation (A4) in that paper)
217 and so $\zeta_{(i, i')} \geq \sum_{k' \in \text{Succ}_{(i, i')}} \text{Vec}_{k'}$ hence (i, i') is pruned by Algorithm 2 and $\mathcal{K} \setminus \mathcal{K}^{\text{pr}} \subseteq \mathcal{K} \setminus \mathcal{L}$.

218 In the end, $\mathcal{K} \setminus \mathcal{K}^{\text{pr}} = \mathcal{K} \setminus \mathcal{L}$ so $\mathcal{K}^{\text{pr}} = \mathcal{L}$. \square \square

Algorithm 2 Pruning of \mathfrak{R}

```

1: procedure PRUNING( $\mathfrak{R} = (R_k, \zeta_k)_{k \in \mathcal{K}}$  with  $\mathfrak{R}$  complete)
2:    $\mathcal{L} \leftarrow \mathcal{K}$ 
3:    $H \leftarrow \max_{k \in \mathcal{K}} \phi(k)$ 
4:   for  $h = H - 1, \dots, 1$  do
5:      $\mathcal{K}^h \leftarrow \{k \in \mathcal{K} : \phi(k) = h\}$ 
6:      $newVec \leftarrow (0)_{k \in \mathcal{K}^h}$ 
7:     for  $k \in \mathcal{K}^h$  do
8:        $Succ_k \leftarrow \{k' \in \mathcal{K}^{h+1} : R_{k'} \subseteq R_k\}$ 
9:       if  $Succ_k = \emptyset$  then
10:         $newVec_k \leftarrow \zeta_k$ 
11:       else
12:         if  $\zeta_k \geq \sum_{k' \in Succ_k} Vec_{k'}$  then
13:            $\mathcal{L} \leftarrow \mathcal{L} \setminus \{k\}$  ▷ pruning of the region indexed by  $k$ 
14:         end if
15:          $newVec_k \leftarrow \min(\zeta_k, \sum_{k' \in Succ_k} Vec_{k'})$ 
16:       end if
17:     end for
18:      $Vec \leftarrow newVec$ 
19:   end for
20:   return  $(\mathcal{L}, \sum_{k \in \mathcal{K}^1} Vec_k)$ 
21: end procedure

```

219 **3.2 Fast algorithm to compute a curve of confidence bounds on a path of selection
220 sets**

221 Let (i_1, \dots, i_m) a permutation of \mathbb{N}_m^* , eventually random, and, for all $t \in \mathbb{N}_m^*$, let $S_t = \{i_1, \dots, i_t\}$ and
222 $S_0 = \emptyset$. For example, (i_1, \dots, i_m) can be the permutation ordering the p -values in increasing order
223 and in that case S_t becomes the set of indices of the t smallest p -values. Assume that we want to
224 compute all $V_{\mathfrak{R}}^*(S_t)$ for all $t \in \{0, \dots, m\}$, this is what we call the curve of confidence bounds indexed
225 by (i_1, \dots, i_m) . Applying Algorithm 1 to compute $V_{\mathfrak{R}}^*(S_t)$ for a given t has complexity $O(t|\mathcal{K}|)$, so using
226 it to sequentially compute the full curve has complexity $O(\sum_{t=0}^m t|\mathcal{K}|) = O(m^2|\mathcal{K}|)$. In this section,
227 we present a new algorithm that computes the curve with a $O(m|\mathcal{K}|)$ complexity. The algorithm
228 will need that \mathfrak{R} is complete, so if that is not the case we first need to complete \mathfrak{R} following the
229 Algorithm 2 of Durand et al. (2020), which has a $O(m|\mathcal{K}|)$ complexity. In the remainder of this section
230 we assume that \mathfrak{R} is complete.

231 We first recall and introduce some notation. Recall that ϕ is the depth function inside of \mathfrak{R} , that
232 $\mathfrak{P} \subseteq \mathcal{P}(\mathcal{K})$ is the set of subsets of \mathcal{K} that realize a partition, recall the important result stated by
233 Equation (12), and that $\mathcal{K}^h = \{k \in \mathcal{K} : \phi(k) = h\}$ for all $1 \leq h \leq H$ where $H = \max_{k \in \mathcal{K}} \phi(k)$. For
234 any $t \in \mathbb{N}_m^*$ and $1 \leq h \leq H$, we denote by $k^{(t,h)}$ the element of \mathcal{K}^h such that $i_t \in R_{k^{(t,h)}}$ if it exists, and
235 we denote by $h_{\max}(t)$ the highest h such that $k^{(t,h)}$ exists.

236 **Example 3.1** (Continuation of Example 2.2 and Example 2.3). Assume that the reference family of
237 Example 2.2 has been labeled as in Example 2.3 and completed. Let (i_1, \dots, i_{25}) such that $i_1 = 7, i_2 = 1$
238 and $i_3 = 24$. Then for $t = 1, k^{(t,1)} = (1, 5), k^{(t,2)} = (2, 3), k^{(t,3)} = (3, 3)$ and $h_{\max}(t) = H = 3$. For $t = 2$,
239 $k^{(t,1)} = (1, 5), k^{(t,2)} = (1, 1), k^{(t,3)}$ does not exist and $h_{\max}(t) = 2$. For $t = 3, k^{(t,1)} = (8, 8), k^{(t,2)}$ does
240 not exist and $h_{\max}(t) = 1$.

241 Now we can finally present the new algorithm and the proof that it computes the curve $(V_{\mathfrak{R}}^*(S_t))_{t \in \mathbb{N}_m}$.
242 We present two versions of the algorithm (strictly equivalent): one very formal (Algorithm 3), to

243 introduce additional notation used in the proof of Theorem 3.1, and, later, a simpler version that is
 244 the one actually implemented (Algorithm 4). Recall that a detailed illustration of the steps of the
 245 algorithms will be provided in Section 3.3.

Algorithm 3 Formal computation of $(V_{\mathfrak{R}}^*(S_t))_{0 \leq t \leq m}$

```

1: procedure CURVE( $\mathfrak{R} = (R_k, \zeta_k)_{k \in \mathcal{K}}$  with  $\mathfrak{R}$  complete, path  $(S_t)_{1 \leq t \leq m}$  with  $S_t = \{i_1, \dots, i_t\}$ 
2:    $\mathcal{P}^0 \leftarrow \{(i, i) : 1 \leq i \leq n\}$  ▷ the set of all atoms indices
3:    $\mathcal{K}_0^- \leftarrow \{k \in \mathcal{K} : \zeta_k = 0\}$ 
4:    $\eta_k^0 \leftarrow 0$  for all  $k \in \mathcal{K}$ 
5:   for  $t = 1, \dots, m$  do
6:     if  $i_t \in \bigcup_{k \in \mathcal{K}_{t-1}^-} R_k$  then
7:        $\mathcal{P}^t \leftarrow \mathcal{P}^{t-1}$ 
8:        $\mathcal{K}_t^- \leftarrow \mathcal{K}_{t-1}^-$ 
9:        $\eta_k^t \leftarrow \eta_k^{t-1}$  for all  $k \in \mathcal{K}$ 
10:    else
11:      for  $h = 1, \dots, h_{\max}(t)$  do
12:         $\eta_{k^{(t,h)}}^t \leftarrow \eta_{k^{(t,h)}}^{t-1} + 1$ 
13:        if  $\eta_{k^{(t,h)}}^t < \zeta_k$  then
14:          Pass
15:        else
16:           $h_t^f \leftarrow h$  ▷ final depth
17:           $\mathcal{P}^t \leftarrow \left( \mathcal{P}^{t-1} \setminus \{k \in \mathcal{P}^{t-1} : R_k \subseteq R_{k^{(t,h_t^f)}}\} \right) \cup \{k^{(t,h_t^f)}\}$ 
18:           $\mathcal{K}_t^- \leftarrow \mathcal{K}_{t-1}^- \cup \{k^{(t,h_t^f)}\}$ 
19:          Break the loop
20:        end if
21:      end for
22:      if the loop has been broken then
23:         $\eta_k^t \leftarrow \eta_k^{t-1}$  for all  $k \in \mathcal{K}$  not visited during the loop, that is all  $k \notin \{k^{(t,h)}, 1 \leq h \leq h_t^f\}$ 
24:      else
25:         $\mathcal{P}^t \leftarrow \mathcal{P}^{t-1}$ 
26:         $\mathcal{K}_t^- \leftarrow \mathcal{K}_{t-1}^-$ 
27:         $\eta_k^t \leftarrow \eta_k^{t-1}$  for all  $k \in \mathcal{K}$  not visited during the loop, that is all  $k \notin \{k^{(t,h)}, 1 \leq h \leq h_{\max}(t)\}$ 
28:      end if
29:    end if
30:  end for
31:  return  $\mathcal{P}^t, \eta_k^t$  for all  $t = 1, \dots, m$  and  $k \in \mathcal{K}$ 
32: end procedure

```

246 The core idea of the algorithm is that, as we increase t and add new hypotheses in S_t , we inflate a
 247 counter η_k^t for each region R_k , by 1 if $i_t \in R_k$ (line 12), by 0 if not (lines 23 and 27), but only until the
 248 counter reaches ζ_k (line 13). After this point, the hypotheses in R_k don't contribute to $V_{\mathfrak{R}}^*(S_t)$, we
 249 keep track of those hypotheses with \mathcal{K}_t^- (line 6), so as soon as $\eta_{k^{(t,h)}}^t = \zeta_k$ we update \mathcal{K}_t^- by adding
 250 $k^{(t,h)}$ (line 18) to it and we update \mathcal{P}^t accordingly (line 17).

251 We will see in the following Theorem 3.1 how this algorithm allows to compute $V_{\mathfrak{R}}^*(S_t)$. We first need
 252 a final notation. Let

$$\mathcal{K}_t = \{k \in \mathcal{K} : \exists k' \in \mathcal{P}^t : R_{k'} \subseteq R_k\}.$$

253 The elements of \mathcal{K}_t index the regions of the forest that “are above” the regions of the current
 254 partition-realizing \mathcal{P}^t . In particular, we always have, for any $t \in \mathbb{N}_m$, $\mathcal{K}^1 \subseteq \mathcal{K}_t$ and $\mathcal{P}^t \subseteq \mathcal{K}_t$. We
 255 can also remark that the sequence $(\mathcal{K}_t)_{0 \leq t \leq m}$ is non-increasing for the inclusion relation, and that
 256 $\mathcal{K}_0 = \mathcal{K}$.

257 **Theorem 3.1** (Fast curve computation). *Let any $t \in \mathbb{N}_m$. Then, $\mathcal{P}^t \in \mathfrak{P}$, and for all $k \in \mathcal{K}_t$, we have*

$$V_{\mathfrak{R}}^*(S_t \cap R_k) = \eta_k^t \quad (16)$$

258 and

$$V_{\mathfrak{R}}^*(S_t \cap R_k) = \sum_{\substack{k' \in \mathcal{P}^t \\ R_{k'} \subseteq R_k}} \zeta_{k'} \wedge |S_t \cap R_{k'}|. \quad (17)$$

259 Furthermore,

$$V_{\mathfrak{R}}^*(S_t) = \sum_{k \in \mathcal{P}^t} \zeta_k \wedge |S_t \cap R_k| = \sum_{k \in \mathcal{K}^1} \eta_k^t. \quad (18)$$

260 The proof of this Theorem is postponed to Section 3.4. The first equality of Equation (18) states that
 261 the minimum in (12) is realized on the partition \mathcal{P}^t , and the last equality of the same Equation is the
 262 basis of the following light corollary.

263 **Corollary 3.1** (Easy computation). *For $t \in \{0, \dots, m-1\}$, $V_{\mathfrak{R}}^*(S_{t+1}) = V_{\mathfrak{R}}^*(S_t)$ if $i_{t+1} \in \bigcup_{k \in \mathcal{K}_t^-} R_k$, and
 264 $V_{\mathfrak{R}}^*(S_{t+1}) = V_{\mathfrak{R}}^*(S_t) + 1$ if not.*

265 *Proof.* From (18), $V_{\mathfrak{R}}^*(S_{t+1}) = \sum_{k \in \mathcal{K}^1} \eta_k^{t+1}$ and $V_{\mathfrak{R}}^*(S_t) = \sum_{k \in \mathcal{K}^1} \eta_k^t$. If $i_{t+1} \in \bigcup_{k \in \mathcal{K}_t^-} R_k$, $\eta_k^{t+1} = \eta_k^t$ for
 266 all $k \in \mathcal{K}^1$. If not, $\eta_k^{t+1} = \eta_k^t$ for all $k \in \mathcal{K}^1$, $k \neq k^{(t+1,1)}$, whereas for $k = k^{(t+1,1)}$, $\eta_k^{t+1} = \eta_k^t + 1$. \square \square

267 We note that, from Theorem 3.1 and Corollary 3.1, if one is only interested in the computation of
 268 the curve $(V_{\mathfrak{R}}^*(S_t))_{1 \leq t \leq m}$, tracking \mathcal{P}^t is actually useless, what is important is to track and update
 269 \mathcal{K}_t^- correctly. Hence the simpler, alternative Algorithm 4. Note that Algorithm 4 is less formal than
 270 Algorithm 3 : as in Algorithm 1 and Algorithm 2, it recycles notation (mimicking the actual code
 271 implementation) so the t subscript or superscript is dropped from the \mathcal{K}_t^- and the η_k^t . In Algorithm 4
 272, the notation V_t is actually equal to $V_{\mathfrak{R}}^*(S_t)$ by Corollary 3.1.

273 It is easy to see that each step t has a complexity in $O(|\mathcal{K}|)$ hence the total complexity is in $O(m|\mathcal{K}|)$.
 274 This is because, if the regions are carefully stocked in memory, especially if their bounds (in terms
 275 of hypothesis index) are stocked, then finding $k^{(t,h)}$ has a complexity in $O(|\mathcal{K}^h|)$ and checking if
 276 $i_t \in \bigcup_{k \in \mathcal{K}_{t-1}^-} R_k$ has a complexity in $O(|\mathcal{K}|)$.

277 3.3 Illustration on a detailed example

278 We still continue Example 2.2 and Example 2.3. Recall that $m = 25$, $P_{1:5} = R_1 = \{1, \dots, 20\}$, $P_1 =$
 279 $R_2 = \{1, 2\}$, $P_{2:3} = R_3 = \{3, \dots, 10\}$, $P_{4:5} = R_4 = \{11, \dots, 20\}$, $P_2 = \{3, 4\}$, $P_3 = R_5 = \{5, \dots, 10\}$,
 280 $P_4 = R_6 = \{11, \dots, 16\}$, $P_5 = R_7 = \{17, \dots, 20\}$, $P_{6:7} = R_8 = \{21, 22\}$, $P_6 = \{21\}$, $P_7 = R_9 = \{22\}$ and
 281 $P_8 = \{23, 24, 25\}$.

282 Now assume that we have the following values for the ζ_k ’s: $\zeta_{(1,5)} = 6$, $\zeta_{(1,1)} = 2$, $\zeta_{(2,3)} = 1$, $\zeta_{(3,3)} = 4$,
 283 $\zeta_{(4,5)} = 4$, $\zeta_{(4,4)} = 2$, $\zeta_{(5,5)} = 3$, $\zeta_{(6,7)} = 2$, $\zeta_{(7,7)} = 0$. Because P_2 , P_6 and P_8 come from the completion
 284 operation (see Section 2.3), we also have $\zeta_{(2,2)} = |P_2| = 2$, $\zeta_{(6,6)} = |P_6| = 1$ and $\zeta_{(8,8)} = |P_8| = 3$. These
 285 values are summarized in Figure 3.

286 We want to compute the curve $(V_{\mathfrak{R}}^*(S_t))_{1 \leq t \leq 9}$ with $S_t = \{i_1, \dots, i_t\}$ and $i_1 = 11$, $i_2 = 17$, $i_3 = 12$, $i_4 = 13$,
 287 $i_5 = 18$, $i_6 = 3$, $i_7 = 19$, $i_8 = 22$ and $i_9 = 5$.

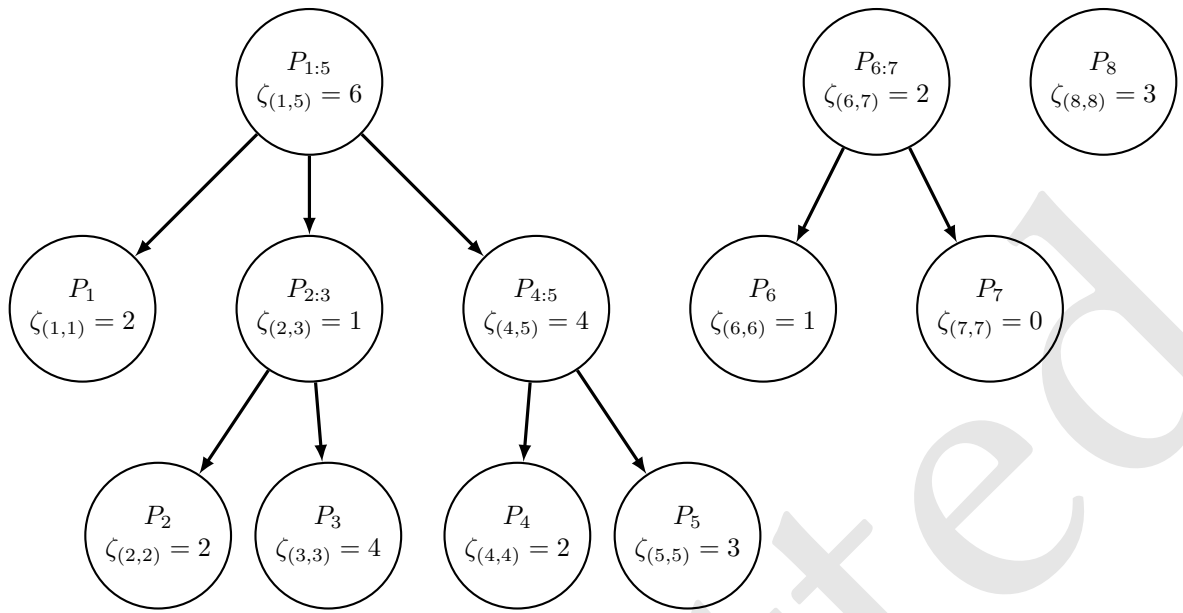


Figure 3: The regions of Example 2.2 with the ζ_k values.

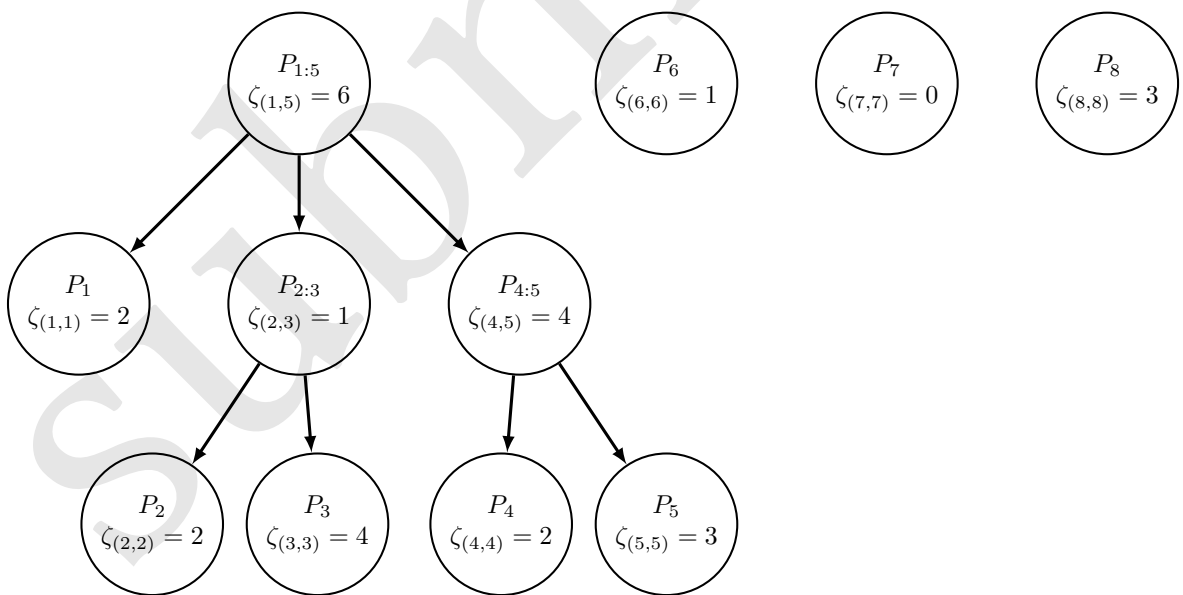


Figure 4: The regions of Example 2.2 after pruning.

Algorithm 4 Practical computation of $(V_{\mathfrak{R}}^*(S_t))_{0 \leq t \leq m}$

```

1: procedure CURVE( $\mathfrak{R} = (R_k, \zeta_k)_{k \in \mathcal{K}}$  with  $\mathfrak{R}$  complete, path  $(S_t)_{1 \leq t \leq m}$  with  $S_t = \{i_1, \dots, i_t\}$ )
2:    $V_0 \leftarrow 0$ 
3:    $\mathcal{K}^- \leftarrow \{k \in \mathcal{K} : \zeta_k = 0\}$ 
4:    $\eta_k \leftarrow 0$  for all  $k \in \mathcal{K}$ 
5:   for  $t = 1, \dots, m$  do
6:     if  $i_t \in \bigcup_{k \in \mathcal{K}^-} R_k$  then
7:        $V_t \leftarrow V_{t-1}$ 
8:     else
9:       for  $h = 1, \dots, h_{\max}(t)$  do
10:        find  $k^{(t,h)} \in \mathcal{K}^h$  such that  $i_t \in R_{k^{(t,h)}}$ 
11:         $\eta_{k^{(t,h)}} \leftarrow \eta_{k^{(t,h)}} + 1$ 
12:        if  $\eta_{k^{(t,h)}} < \zeta_k$  then
13:          pass
14:        else
15:           $\mathcal{K}^- \leftarrow \mathcal{K}^- \cup \{k^{(t,h)}\}$ 
16:          break the loop
17:        end if
18:      end for
19:       $V_t \leftarrow V_{t-1} + 1$ 
20:    end if
21:  end for
22:  return  $(V_t)_{1 \leq t \leq m}$ 
23: end procedure

```

288 First, we apply Algorithm 2 to the family. This results in pruning $P_{6:7}$ (and only this region), because
289 $2 = \zeta_{(6,7)} \geq \zeta_{(6,6)} + \zeta_{(7,7)} = 1 + 0$. This gives Figure 4.

290 Now we initialize Algorithm 3, that is we let $t = 0$. Because $\zeta_{(7,7)} = 0$, $(7,7)$ is added to \mathcal{K}_t^- :
291 $\mathcal{K}_0^- = \{(7,7)\}$. Furthermore, all η_k^t are set to 0. The initial state of Algorithm 3 is shown in Figure 5,
292 with $(7,7)$ being in red to show that it will not contribute to the computations.

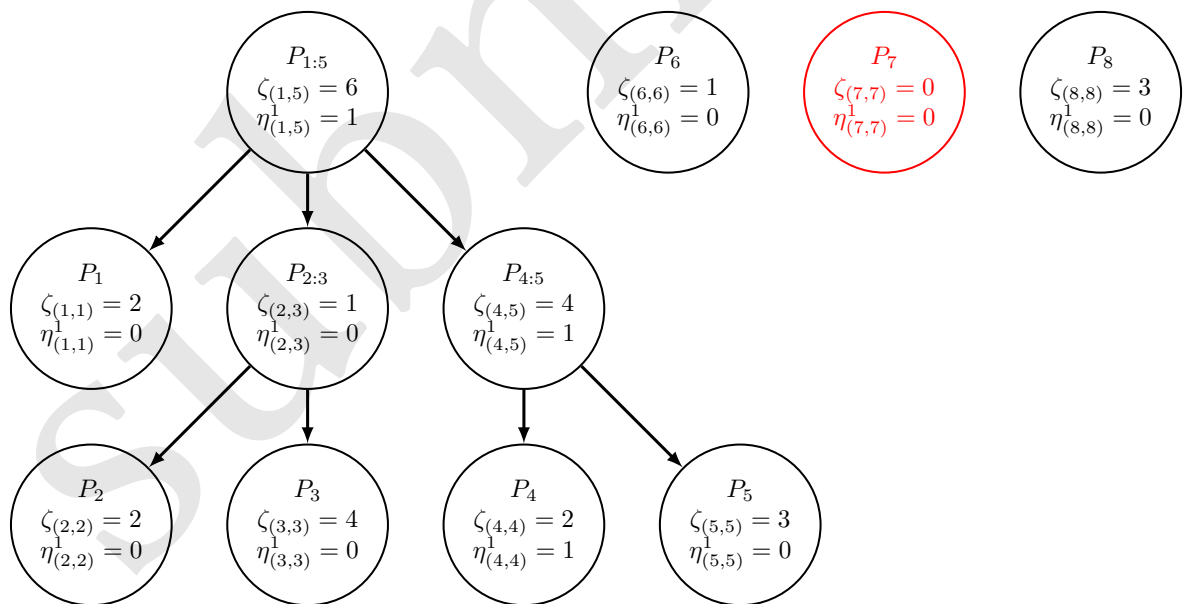
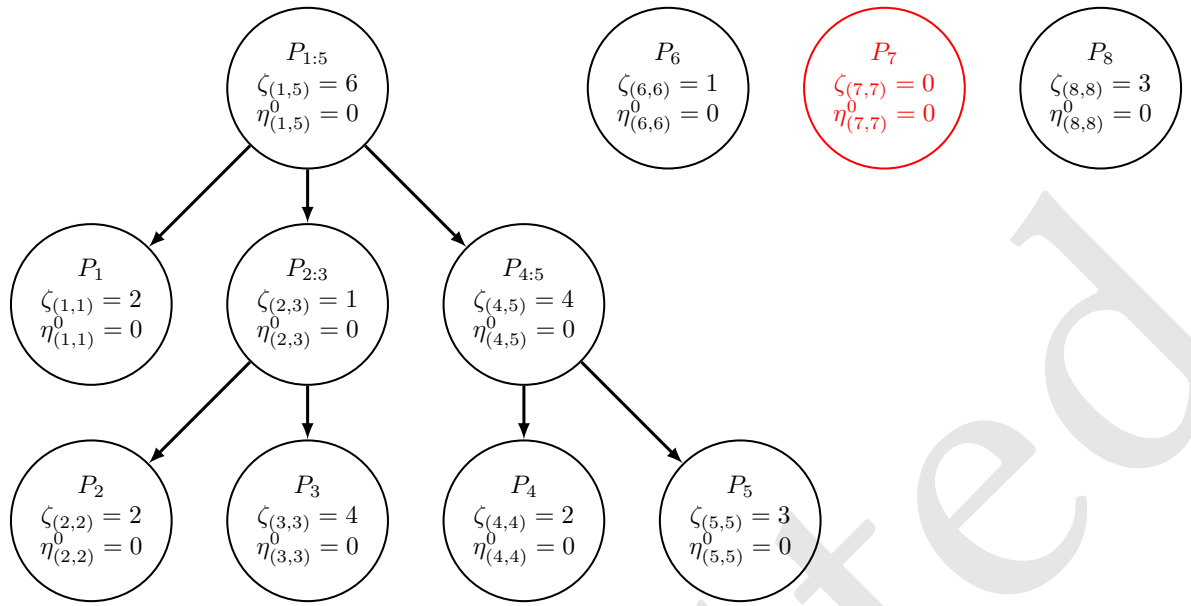
293 We move on to $t = 1$, with $i_1 = 11$. $i_1 \in P_4 \subseteq P_{4:5} \subseteq P_{1:5}$. The appropriate η_k^t are increased by one,
294 and by (18) we have $V_{\mathfrak{R}}^*(S_1) = \eta_{(1,5)}^1 + \eta_{(6,6)}^1 + \eta_{(7,7)}^1 + \eta_{(8,8)}^1 = 1 + 0 + 0 + 0 = 1$. The state of the step
295 is summarized in Figure 6.

296 We move on to $t = 2$, with $i_2 = 17$. $i_1 \in P_5 \subseteq P_{4:5} \subseteq P_{1:5}$. The appropriate η_k^t are increased by one,
297 and by (18) we have $V_{\mathfrak{R}}^*(S_2) = 2$. The state of the step is summarized in Figure 7.

298 We move on to $t = 3$, with $i_3 = 12$. $i_3 \in P_4 \subseteq P_{4:5} \subseteq P_{1:5}$. The appropriate η_k^t are increased by one, and
299 we notice that $\eta_{(4,4)}^3 = 2 = \zeta_{(4,4)}$. So P_4 will stop contributing, we add it to \mathcal{K}_t^- : $\mathcal{K}_3^- = \{(4,4), (7,7)\}$.
300 By (18), we have $V_{\mathfrak{R}}^*(S_3) = 3$. The state of the step is summarized in Figure 8, with P_4 now also in red.

301 We move on to $t = 4$, with $i_4 = 13$. $i_4 \in P_4 \in \bigcup_{k \in \mathcal{K}_3^-} R_k$. No η_k^t is increased (see line 9 of Algorithm 3
302), and by (18), we have $V_{\mathfrak{R}}^*(S_4) = 3$.

303 We move on to $t = 5$, with $i_5 = 18$. $i_5 \in P_5 \subseteq P_{4:5} \subseteq P_{1:5}$. We first increase $\eta_{(1,5)}^t$: $\eta_{(1,5)}^5 = 4 < \zeta_{(1,5)}$,
304 then $\eta_{(4,5)}^t$: $\eta_{(4,5)}^5 = 4$, and we stop there because $\eta_{(4,5)}^5 = 4 = \zeta_{(4,5)}$. $P_{4:5}$ will stop contributing, we
305 add it to \mathcal{K}_t^- : $\mathcal{K}_5^- = \{(4,5), (4,4), (7,7)\}$. Note that $\eta_{(5,5)}^t$ is not updated because we stopped the loop
306 before, see line 23 of Algorithm 3. By (18), we have $V_{\mathfrak{R}}^*(S_5) = 4$. The state of the step is summarized
307 in Figure 9, with $P_{4:5}$ now also in red.



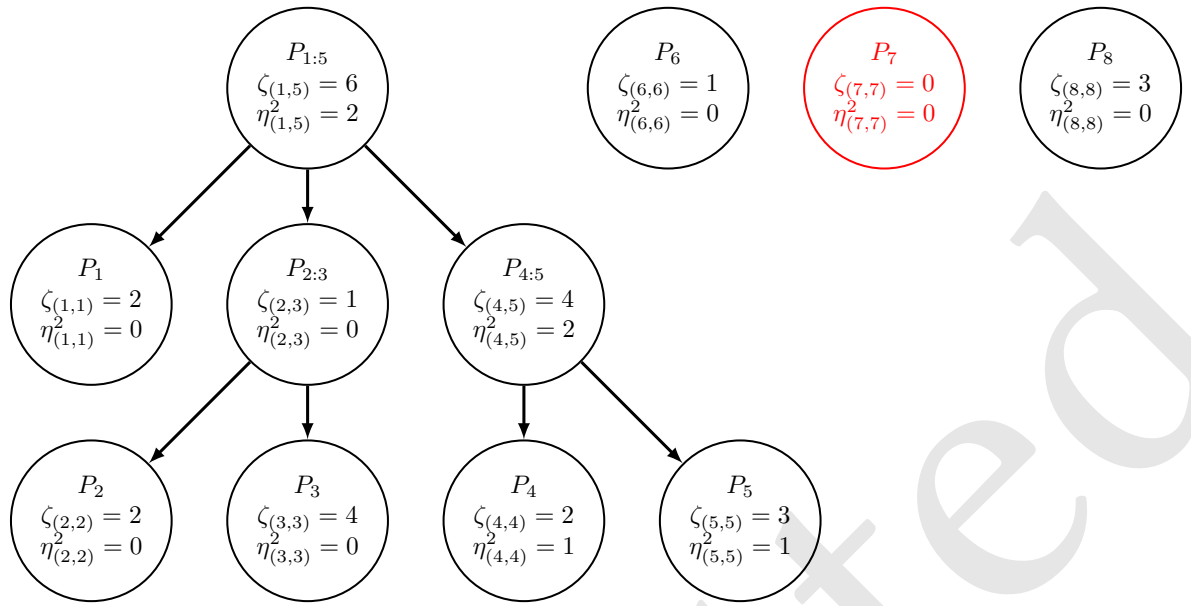


Figure 7: The regions of Example 2.2 at $t = 2$ in Algorithm 3 .

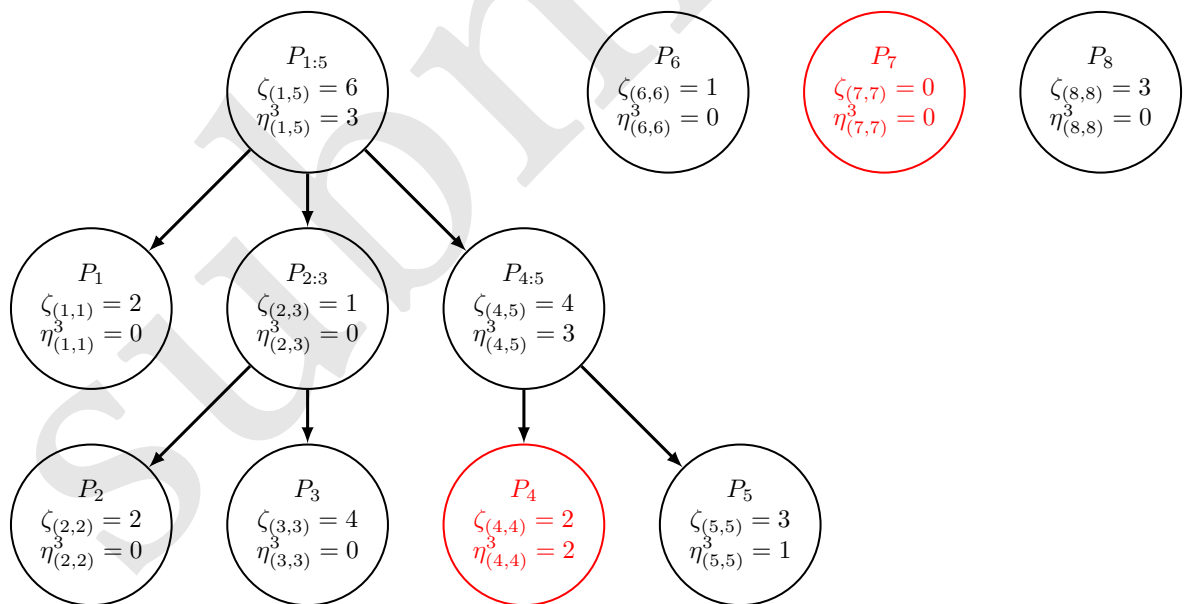


Figure 8: The regions of Example 2.2 at $t = 3$ in Algorithm 3 .

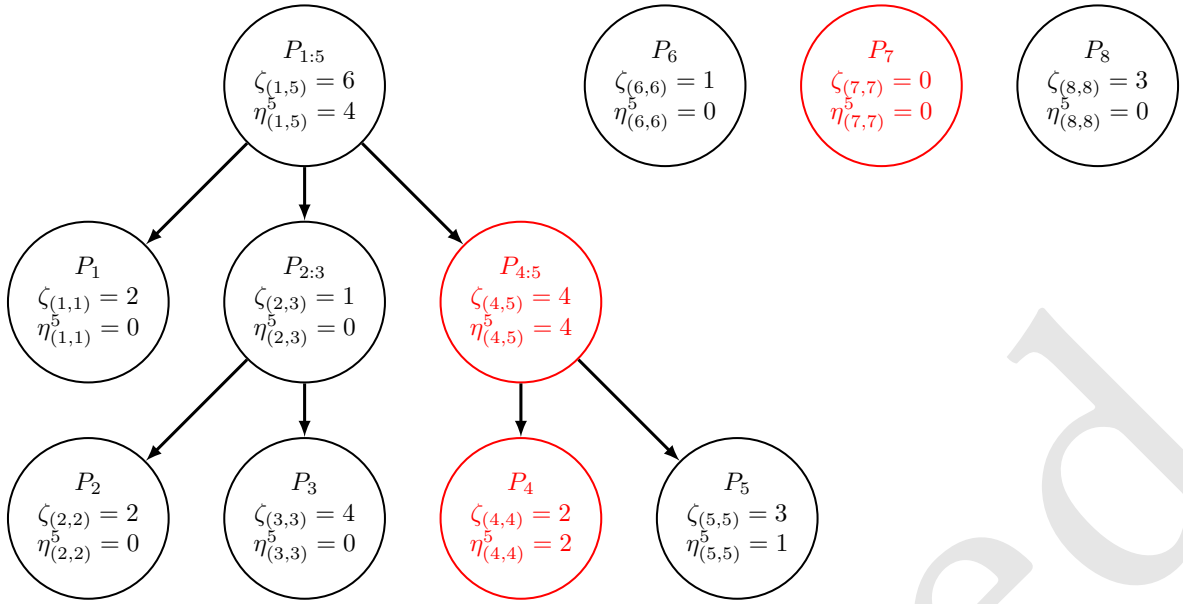


Figure 9: The regions of Example 2.2 at $t = 5$ in Algorithm 3.

308 We move on to $t = 6$, with $i_6 = 3$. $i_6 \in P_3 \subseteq P_{2:3} \subseteq P_{1:5}$. We first increase $\eta_{(1,5)}^t$: $\eta_{(1,5)}^6 = 5 < \zeta_{(1,5)}$,
 309 then $\eta_{(2,3)}^t$: $\eta_{(2,3)}^6 = 1$, and we stop there because $\eta_{(2,3)}^6 = 1 = \zeta_{(2,3)}$. $P_{2:3}$ will stop contributing, we
 310 add it to \mathcal{K}_t^- : $\mathcal{K}_6^- = \{(2,3), (4,5), (4,4), (7,7)\}$. Note that $\eta_{(3,3)}^t$ is not updated because we stopped
 311 the loop before, see line 23 of Algorithm 3. By (18), we have $V_{\mathfrak{R}}^*(S_6) = 5$. The state of the step is
 312 summarized in Figure 10, with $P_{2:3}$ now also in red.

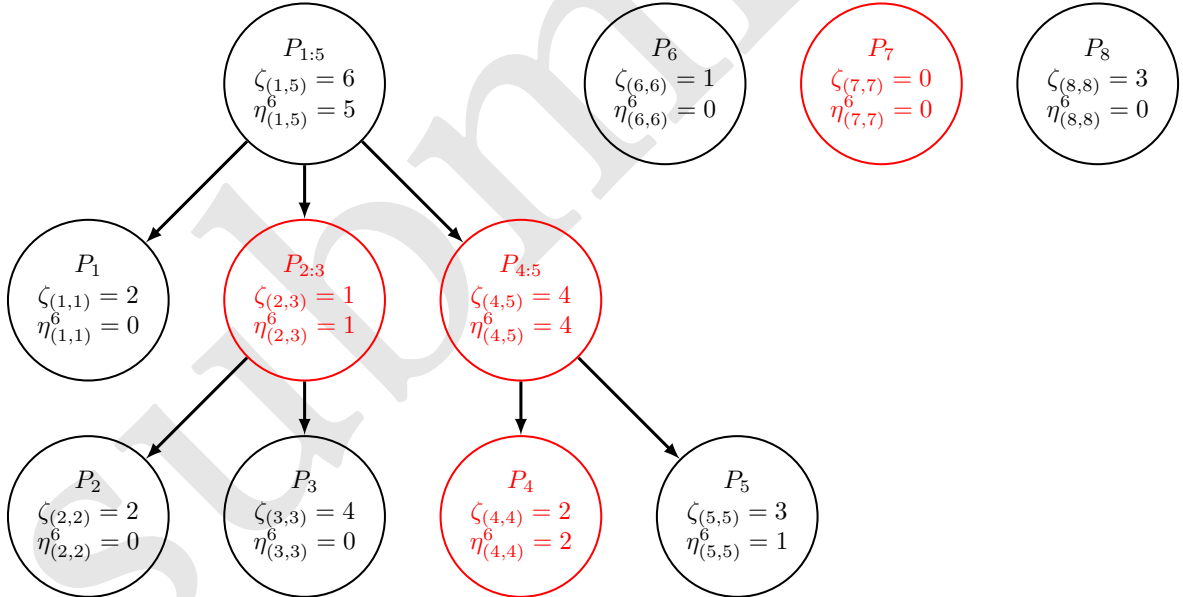


Figure 10: The regions of Example 2.2 at $t = 6$ in Algorithm 3.

313 We move on to the remaining steps. $i_7 = 19 \in P_{4:5}$, $i_8 = 22 \in P_7$ and $i_9 = 5 \in P_{2:3}$ are all
 314 in $\bigcup_{k \in \mathcal{K}_6^-} R_k$ so no η_k^t is increased at their step (see line 9 of Algorithm 3), and by (18), we have
 315 $V_{\mathfrak{R}}^*(S_7) = V_{\mathfrak{R}}^*(S_8) = V_{\mathfrak{R}}^*(S_9) = 5$.

316 **3.4 Proof of Theorem 3.1**

317 **3.4.1 Derivation of (18)**

318 We first derive (18) from (16) and (17). First note that for all $Q \in \mathfrak{P}$,

$$Q = \bigcup_{k \in \mathcal{K}^1} \{k' \in Q : R_{k'} \subseteq R_k\} \quad (19)$$

319 and the union is disjoint. From (12), let $Q^* \in \mathfrak{P}$ such that $V_{\mathfrak{R}}^*(S_t) = \sum_{k' \in Q^*} \zeta_{k'} \wedge |S_t \cap R_{k'}|$. Then by
320 (19),

$$\begin{aligned} V_{\mathfrak{R}}^*(S_t) &= \sum_{k' \in Q^*} \zeta_{k'} \wedge |S_t \cap R_{k'}| \\ &= \sum_{k \in \mathcal{K}^1} \sum_{\substack{k' \in Q^* \\ R_{k'} \subseteq R_k}} \zeta_{k'} \wedge |S_t \cap R_{k'}| \\ &= \sum_{k \in \mathcal{K}^1} \sum_{\substack{k' \in Q^* \\ R_{k'} \subseteq R_k}} \zeta_{k'} \wedge |S_t \cap (R_k \cap R_{k'})| \\ &= \sum_{k \in \mathcal{K}^1} \sum_{k' \in Q^*} \zeta_{k'} \wedge |(S_t \cap R_k) \cap R_{k'}| \end{aligned} \quad (20)$$

$$\geq \sum_{k \in \mathcal{K}^1} V_{\mathfrak{R}}^*(S_t \cap R_k), \quad (21)$$

321 where the equality in (20) comes from the fact that if $R_{k'} \not\subseteq R_k$, then $R_{k'} \cap R_k = \emptyset$, that is, $R_k \subseteq R_{k'}$ is
322 impossible because $k \in \mathcal{K}^1$. Furthermore, (21) holds again by (12).

323 Because $\mathcal{K}^1 \subseteq \mathcal{K}_t$, by (17), $V_{\mathfrak{R}}^*(S_t \cap R_k) = \sum_{\substack{k' \in \mathcal{P}^t \\ R_{k'} \subseteq R_k}} \zeta_{k'} \wedge |S_t \cap R_{k'}|$ for all $k \in \mathcal{K}^1$. Then,

$$\begin{aligned} \sum_{k \in \mathcal{K}^1} V_{\mathfrak{R}}^*(S_t \cap R_k) &= \sum_{k \in \mathcal{K}^1} \sum_{\substack{k' \in \mathcal{P}^t \\ R_{k'} \subseteq R_k}} \zeta_{k'} \wedge |S_t \cap R_{k'}| \\ &= \sum_{k \in \mathcal{P}^t} \zeta_k \wedge |S_t \cap R_k| \text{ by (19)} \\ &\geq V_{\mathfrak{R}}^*(S_t) \text{ by (12).} \end{aligned}$$

324 So we proved that $V_{\mathfrak{R}}^*(S_t) = \sum_{k \in \mathcal{P}^t} \zeta_k \wedge |S_t \cap R_k| = \sum_{k \in \mathcal{K}^1} V_{\mathfrak{R}}^*(S_t \cap R_k)$ and finally $V_{\mathfrak{R}}^*(S_t) =$
325 $\sum_{k \in \mathcal{K}^1} V_{\mathfrak{R}}^*(S_t \cap R_k) = \sum_{k \in \mathcal{K}^1} \eta_k^t$ by (16), again because $\mathcal{K}^1 \subseteq \mathcal{K}_t$. Every equality in (18) is proven.

326 **3.4.2 Proof of (16) and (17)**

327 We show the remainder of the statements by a strong recursion over t . We have $\mathcal{P}^0 \in \mathfrak{P}$ by definition,
328 and given that $S_0 = \emptyset$ and $\eta_k^0 = 0$ for all $k \in \mathcal{K}$ (recall that $\mathcal{K}_0 = \mathcal{K}$), everything is equal to 0 in (16)
329 and (17).

330 So we let $t \in \{0, \dots, m-1\}$, and assume that $\mathcal{P}^{t'} \in \mathfrak{P}$ and that (16) and (17) hold for all $t' \leq t$.
331 In all the following, \bar{k} is the element of \mathcal{P}^t such that $i_{t+1} \in R_{\bar{k}}$. We will distinguish two cases: if
332 $i_{t+1} \in \bigcup_{k \in \mathcal{K}_t^-} R_k$ or not. First we show an inequality that will be used in both cases. We have, for all
333 $k \in \mathcal{K}_t$,

$$V_{\mathfrak{R}}^*(S_{t+1} \cap R_k) \leq \sum_{\substack{k' \in \mathcal{P}^t \\ R_{k'} \subseteq R_k}} \zeta_{k'} \wedge |S_{t+1} \cap R_{k'}|. \quad (22)$$

334 Indeed, by (12),

$$V_{\mathfrak{R}}^*(S_{t+1} \cap R_k) \leq \sum_{k' \in \mathcal{P}^t} \zeta_{k'} \wedge |S_{t+1} \cap R_k \cap R_{k'}|.$$

335 For any $k' \in \mathcal{P}^t$, we have either $R_{k'} \cap R_k = \emptyset$, in which case $|S_{t+1} \cap R_k \cap R_{k'}| = 0$, either $R_{k'} \subseteq R_k$,
 336 in which case $|S_{t+1} \cap R_k \cap R_{k'}| = |S_{t+1} \cap R_{k'}|$, but $R_k \subsetneq R_{k'}$ is impossible. Indeed, by definition of \mathcal{K}_t ,
 337 there exists $\tilde{k} \in \mathcal{P}^t$ such that $R_{\tilde{k}} \subseteq R_k$, so $R_k \subsetneq R_{k'}$ would entail $R_{\tilde{k}} \subsetneq R_{k'}$ which is impossible since
 338 $k', \tilde{k} \in \mathcal{P}^t \in \mathfrak{P}$ and so $R_{\tilde{k}}$ and $R_{k'}$ are part of a partition of \mathbb{N}_m^* . This gives (22).

339 **3.4.2.1 First case:** $i_{t+1} \in \bigcup_{k \in \mathcal{K}_t^-} R_k$

340 In this case, $\mathcal{P}^{t+1} = \mathcal{P}^t \in \mathfrak{P}$ and $\mathcal{K}_{t+1} = \mathcal{K}_t$. For any $k \in \mathcal{K}_{t+1}$ such that $i_{t+1} \notin R_k$ (or, equivalently,
 341 such that $S_{t+1} \cap R_k = S_t \cap R_k$),

$$\begin{aligned} \sum_{\substack{k' \in \mathcal{P}^{t+1} \\ R_{k'} \subseteq R_k}} \zeta_{k'} \wedge |S_{t+1} \cap R_{k'}| &= \sum_{\substack{k' \in \mathcal{P}^t \\ R_{k'} \subseteq R_k}} \zeta_{k'} \wedge |S_t \cap R_{k'}| \\ &= V_{\mathfrak{R}}^*(S_t \cap R_k) \text{ by (17)} \\ &= \eta_k^t \text{ by (16)} \\ &= \eta_k^{t+1} \end{aligned}$$

342 because $\eta_k^t = \eta_k^{t+1}$ for all $k \in \mathcal{K}$. Furthermore $S_{t+1} \cap R_k = S_t \cap R_k$ so $V_{\mathfrak{R}}^*(S_{t+1} \cap R_k) = V_{\mathfrak{R}}^*(S_t \cap R_k)$. So
 343 everything is proved for such a k .

344 Now we let $k \in \mathcal{K}_{t+1}$ such that $i_{t+1} \in R_k$ or, equivalently, such that $R_{\tilde{k}} \subseteq R_k$. We first need to show
 345 that $\zeta_{\tilde{k}} \leq |S_t \cap R_{\tilde{k}}|$, and for that we need to distinguish two subcases: if \tilde{k} has been added to \mathcal{P}^t during
 346 a previous step of the algorithm, or if not.

347 **3.4.2.1.1 First subcase: \tilde{k} has never been added during the process of line 17**

348 Then $\tilde{k} \in \mathcal{P}^0$ and $R_{\tilde{k}}$ is an atom, so $i_{t+1} \in \bigcup_{k' \in \mathcal{K}_t^-} R_{k'}$ implies that $R_{\tilde{k}} \subseteq \bigcup_{k' \in \mathcal{K}_t^-} R_{k'}$ (because of the
 349 forest structure). Let k'_{\max} such that

$$R_{k'_{\max}} = \max\{R_{k'} : k' \in \mathcal{K}_t^-, R_{\tilde{k}} \subseteq R_{k'}\}$$

350 (this a maximum for the inclusion relation, and it is well defined thanks to the forest structure). By
 351 reductio ad absurdum we show that $k'_{\max} = \tilde{k}$. If that wasn't the case, by the joint construction of
 352 \mathcal{P}^t and \mathcal{K}_t^- during the algorithm we would have $k'_{\max} \in \mathcal{P}^t$ and a contradiction with the fact that
 353 $\mathcal{P}^t \in \mathfrak{P}$: we can't have both $\tilde{k} \in \mathcal{P}^t$ and $k'_{\max} \in \mathcal{P}^t$ if they are distinct. So $k'_{\max} = \tilde{k}$, so $\tilde{k} \in \mathcal{K}_t^-$, but
 354 it cannot have been added to \mathcal{K}_t^- during a previous step of the algorithm, otherwise it would have
 355 been added to \mathcal{P}^t , too. Hence $\tilde{k} \in \mathcal{K}_0^-$ which means that $\zeta_{\tilde{k}} = 0$ and $\zeta_{\tilde{k}} = 0 \leq |S_t \cap R_{\tilde{k}}|$.

356 **3.4.2.1.2 Second subcase: \tilde{k} has been added to \mathcal{P}^t at a previous step**

357 Let $t' \leq t$ be this step. This means that $\tilde{k} = k^{(t', h_{t'})}$ and that at that step $\eta_{\tilde{k}}^{t'} = \zeta_{\tilde{k}}$. Indeed, the if
 358 condition in line 13 failed so $\eta_{\tilde{k}}^{t'} \geq \zeta_{\tilde{k}}$, but for all $t'' < t'$ we had $\eta_{\tilde{k}}^{t''} \leq \zeta_{\tilde{k}}$ which implies equality. Also
 359 $\tilde{k} \in \mathcal{P}^{t'}$ so $\tilde{k} \in \mathcal{K}_{t'}$ so we can write

$$\begin{aligned} \zeta_{\tilde{k}} &= \eta_{\tilde{k}}^{t'} \\ &= V_{\mathfrak{R}}^*(S_{t'} \cap R_{\tilde{k}}) \text{ by (16)} \\ &\leq |S_{t'} \cap R_{\tilde{k}}| \\ &\leq |S_t \cap R_{\tilde{k}}|. \end{aligned}$$

360 This concludes the two subcases dichotomy: $\zeta_{\bar{k}} \leq |S_t \cap R_{\bar{k}}|$ and we can go back to our $k \in \mathcal{K}_{t+1}$ such
361 that $i_{t+1} \in R_k$ and $R_{\bar{k}} \subseteq R_k$.

362 We write the following chain:

$$\begin{aligned}
V_{\mathfrak{R}}^*(S_{t+1} \cap R_k) &\leq \sum_{\substack{k' \in \mathcal{P}^t \\ R_{k'} \subseteq R_k}} \zeta_{k'} \wedge |S_{t+1} \cap R_{k'}| \text{ by (22) and } \mathcal{K}_{t+1} \subseteq \mathcal{K}_t \\
&= \sum_{\substack{k' \in \mathcal{P}^t \\ R_{k'} \subseteq R_k \\ k' \neq \bar{k}}} \zeta_{k'} \wedge |S_{t+1} \cap R_{k'}| + \zeta_{\bar{k}} \wedge |S_{t+1} \cap R_{\bar{k}}| \\
&= \sum_{\substack{k' \in \mathcal{P}^t \\ R_{k'} \subseteq R_k \\ k' \neq \bar{k}}} \zeta_{k'} \wedge |S_t \cap R_{k'}| + \zeta_{\bar{k}} \wedge (|S_t \cap R_{\bar{k}}| + 1) \\
&= \sum_{\substack{k' \in \mathcal{P}^t \\ R_{k'} \subseteq R_k \\ k' \neq \bar{k}}} \zeta_{k'} \wedge |S_t \cap R_{k'}| + \zeta_{\bar{k}} \wedge |S_t \cap R_{\bar{k}}| \text{ because } \zeta_{\bar{k}} \leq |S_t \cap R_{\bar{k}}| \\
&= \sum_{\substack{k' \in \mathcal{P}^t \\ R_{k'} \subseteq R_k \\ k' \neq \bar{k}}} \zeta_{k'} \wedge |S_t \cap R_{k'}| \\
&= V_{\mathfrak{R}}^*(S_t \cap R_k) \text{ by (17)} \\
&= \eta_k^t \text{ by (16)} \\
&= \eta_k^{t+1}.
\end{aligned}$$

363 But on the other hand, $S_t \subseteq S_{t+1}$ and so (12) also gives $V_{\mathfrak{R}}^*(S_t \cap R_k) \leq V_{\mathfrak{R}}^*(S_{t+1} \cap R_k)$ and so in the end
364 we have the desired outcome:

$$V_{\mathfrak{R}}^*(S_{t+1} \cap R_k) = \eta_k^{t+1} = \sum_{\substack{k' \in \mathcal{P}^{t+1} \\ R_{k'} \subseteq R_k}} \zeta_{k'} \wedge |S_{t+1} \cap R_{k'}|,$$

365 which concludes this first case.

366 3.4.2.2 Second case: $i_{t+1} \notin \bigcup_{k \in \mathcal{K}_t^-} R_k$

367 We first prove that $\mathcal{P}^{t+1} \in \mathfrak{P}$ whether it came from the adjustment in line 17 or not. If it didn't, it
368 stayed equal to $\mathcal{P}^t \in \mathfrak{P}$. If it did, we have

$$\mathcal{P}^{t+1} = \left(\mathcal{P}^t \setminus \{k \in \mathcal{P}^t, R_k \subseteq R_{k^{(t+1,h_{t+1}^f)}}\} \right) \cup \{k^{(t+1,h_{t+1}^f)}\}. \quad (23)$$

369 To prove that $\mathcal{P}^{t+1} \in \mathfrak{P}$ in that case, it suffices to prove there are no $k' \in \mathcal{P}^t$ such that $R_{k^{(t+1,h_{t+1}^f)}} \subsetneq R_{k'}$.
370 If it was the case, because of the strict inclusion, we would have $k' \notin \mathcal{P}^0$, so k' would have been
371 added to $\mathcal{P}^{t'}$ at a previous step $t' \leq t$ of the algorithm, but in that case it would also have been added
372 to $\mathcal{K}_{t'}^- \subseteq \mathcal{K}_t^-$. So in the end we would have

$$i_{t+1} \in R_{k^{(t+1,h_{t+1}^f)}} \subsetneq R_{k'} \subseteq \bigcup_{k \in \mathcal{K}_t^-} R_k$$

373 which is a contradiction and so $\mathcal{P}^{t+1} \in \mathfrak{P}$.

374 Like in the first case, considering a $k \in \mathcal{K}_{t+1} \subseteq \mathcal{K}_t$ such that $i_{t+1} \notin R_k$ is not problematic, because in
 375 that case k is not visited at all by the algorithm at step $t+1$: $\eta_k^{t+1} = \eta_k^t, \{k' \in \mathcal{P}^{t+1} : R_{k'} \subseteq R_k\} =$
 376 $\{k' \in \mathcal{P}^t : R_{k'} \subseteq R_k\}$, and for all $k' \in \mathcal{K}$ such that $R_{k'} \subseteq R_k, S_{t+1} \cap R_{k'} = S_t \cap R_{k'}$. Hence, from

$$V_{\mathfrak{R}}^*(S_t \cap R_k) = \eta_k^t = \sum_{\substack{k' \in \mathcal{P}^t \\ R_{k'} \subseteq R_k}} \zeta_{k'} \wedge |S_{t+1} \cap R_{k'}|,$$

377 we directly have

$$V_{\mathfrak{R}}^*(S_{t+1} \cap R_k) = \eta_k^{t+1} = \sum_{\substack{k' \in \mathcal{P}^{t+1} \\ R_{k'} \subseteq R_k}} \zeta_{k'} \wedge |S_{t+1} \cap R_{k'}|.$$

378 So we now focus on the $k \in \mathcal{K}_{t+1}$ such that $i_{t+1} \in R_k$. Note that for such k ,

$$\eta_k^{t+1} = \eta_k^t + 1 = V_{\mathfrak{R}}^*(S_t \cap R_k) + 1 = \sum_{\substack{k' \in \mathcal{P}^t \\ R_{k'} \subseteq R_k}} \zeta_{k'} \wedge |S_t \cap R_{k'}| + 1$$

379 by construction, by (16) and by (17). Indeed, such a k is equal to a $k^{(t+1,h)}$ with $h \leq h_{\max}(t+1)$, and
 380 even $h \leq h_{t+1}^f$ if the latter exists.

381 Also, similarly to the first case, for all $k \in \mathcal{K}_{t+1}$ such that $i_{t+1} \in R_k$ (recall that this is equivalent to
 382 $R_{\bar{k}} \subseteq R_k$), we can write:

$$\begin{aligned} V_{\mathfrak{R}}^*(S_{t+1} \cap R_k) &\leq \sum_{\substack{k' \in \mathcal{P}^t \\ R_{k'} \subseteq R_k}} \zeta_{k'} \wedge |S_{t+1} \cap R_{k'}| \text{ by (22) and } \mathcal{K}_{t+1} \subseteq \mathcal{K}_t \\ &= \sum_{\substack{k' \in \mathcal{P}^t \\ R_{k'} \subseteq R_k \\ k' \neq \bar{k}}} \zeta_{k'} \wedge |S_{t+1} \cap R_{k'}| + \zeta_{\bar{k}} \wedge |S_{t+1} \cap R_{\bar{k}}| \\ &= \sum_{\substack{k' \in \mathcal{P}^t \\ R_{k'} \subseteq R_k \\ k' \neq \bar{k}}} \zeta_{k'} \wedge |S_t \cap R_{k'}| + \zeta_{\bar{k}} \wedge (|S_t \cap R_{\bar{k}}| + 1) \\ &\leq \sum_{\substack{k' \in \mathcal{P}^t \\ R_{k'} \subseteq R_k \\ k' \neq \bar{k}}} \zeta_{k'} \wedge |S_t \cap R_{k'}| + \zeta_{\bar{k}} \wedge |S_t \cap R_{\bar{k}}| + 1 \\ &= \sum_{\substack{k' \in \mathcal{P}^t \\ R_{k'} \subseteq R_k}} \zeta_{k'} \wedge |S_t \cap R_{k'}| + 1 \\ &= V_{\mathfrak{R}}^*(S_t \cap R_k) + 1 \text{ by (17).} \end{aligned} \tag{24}$$

383 Note that by the joint construction of \mathcal{K}_t^- and \mathcal{P}^t on lines 17 and 18, the fact that $i_{t+1} \notin \bigcup_{k \in \mathcal{K}_t^-} R_k$
 384 implies that \bar{k} is the index of an atom, so actually $h_{\max}(t+1) = \phi(\bar{k}), \bar{k} = k^{(t+1, \phi(\bar{k}))}$ and the R_k ,
 385 $k \in \mathcal{K}_t$, such that $R_{\bar{k}} \subseteq R_k$ are nested and are exactly indexed by the $k^{(t+1,h)}$, $1 \leq h \leq \phi(\bar{k})$. We now
 386 prove that for all of them, $V_{\mathfrak{R}}^*(S_{t+1} \cap R_k) \geq V_{\mathfrak{R}}^*(S_t \cap R_k) + 1$, which will be true in particular for the
 387 ones that are in \mathcal{K}_{t+1} , given that $\mathcal{K}_{t+1} \subseteq \mathcal{K}_t$. We do that by constructing some sets A_h with good
 388 properties with a descending recursion on h , starting from $\phi(\bar{k})$. We only give the first two steps of
 389 the construction, because every other step is exactly the same as the second one, which contains the
 390 recursive arguments. We go back to the real definition of $V_{\mathfrak{R}}^*$ to do so, for any $S \subseteq \mathbb{N}_m$:

$$V_{\mathfrak{R}}^*(S) = \max_{\substack{A \subseteq \mathbb{N}_m \\ \forall k' \in \mathcal{K}, |A \cap R_{k'}| \leq \zeta_{k'}}} |A \cap S| = \max_{\substack{A \subseteq S \\ \forall k' \in \mathcal{K}, |A \cap R_{k'}| \leq \zeta_{k'}}} |A|. \tag{25}$$

391 By (25), we have that $V_{\mathfrak{R}}^*(S_t \cap R_{k^{(t+1,\phi(\bar{k}))}}) = |A_{\phi(\bar{k})}|$ for a given $A_{\phi(\bar{k})} \subseteq S_t \cap R_{k^{(t+1,\phi(\bar{k}))}}$ and such that
 392 $|A_{\phi(\bar{k})} \cap R_{k'}| \leq \zeta_{k'}$ for all $k' \in \mathcal{K}$. Now for the second set, we construct $A_{\phi(\bar{k})-1}$. Note that $V_{\mathfrak{R}}^*(S_t \cap R_{k^{(t+1,\phi(\bar{k})-1)}}) = |B|$ for some $B \subseteq S_t \cap R_{k^{(t+1,\phi(\bar{k})-1)}}$ and such that $|B \cap R_{k'}| \leq \zeta_{k'}$ for all $k' \in \mathcal{K}$. By reductio
 393 ad absurdum, if there are strictly less than $V_{\mathfrak{R}}^*(S_t \cap R_{k^{(t+1,\phi(\bar{k})-1)}}) - V_{\mathfrak{R}}^*(S_t \cap R_{k^{(t+1,\phi(\bar{k}))}}) = |B| - |A_{\phi(\bar{k})}|$
 394 elements in $S_t \cap R_{k^{(t+1,\phi(\bar{k})-1)}} \setminus S_t \cap R_{k^{(t+1,\phi(\bar{k}))}}$, then $|B| + |S_t \cap R_{k^{(t+1,\phi(\bar{k}))}}| - |S_t \cap R_{k^{(t+1,\phi(\bar{k})-1)}}| > |A_{\phi(\bar{k})}| =$
 395 $V_{\mathfrak{R}}^*(S_t \cap R_{k^{(t+1,\phi(\bar{k}))}})$. Given that $B \cup (S_t \cap R_{k^{(t+1,\phi(\bar{k}))}}) \subseteq S_t \cap R_{k^{(t+1,\phi(\bar{k})-1)}}$, this entails $|B \cap S_t \cap R_{k^{(t+1,\phi(\bar{k}))}}| =$
 396 $|B| + |S_t \cap R_{k^{(t+1,\phi(\bar{k}))}}| - |B \cup (S_t \cap R_{k^{(t+1,\phi(\bar{k}))}})| > V_{\mathfrak{R}}^*(S_t \cap R_{k^{(t+1,\phi(\bar{k}))}})$ which contradicts the maximality of
 397 $A_{\phi(\bar{k})}$ in (25).
 398

399 So we construct $A_{\phi(\bar{k})-1}$ by taking the disjoint union of $A_{\phi(\bar{k})}$ and $V_{\mathfrak{R}}^*(S_t \cap R_{k^{(t+1,\phi(\bar{k})-1)}}) - V_{\mathfrak{R}}^*(S_t \cap R_{k^{(t+1,\phi(\bar{k}))}})$
 400 elements of $S_t \cap R_{k^{(t+1,\phi(\bar{k})-1)}} \setminus S_t \cap R_{k^{(t+1,\phi(\bar{k}))}}$. We now establish the properties of $A_{\phi(\bar{k})-1}$. First, $A_{\phi(\bar{k})-1} \subseteq$
 401 $S_t \cap R_{k^{(t+1,\phi(\bar{k})-1)}}$, and $|A_{\phi(\bar{k})-1}| = V_{\mathfrak{R}}^*(S_t \cap R_{k^{(t+1,\phi(\bar{k})-1)}})$. For all $k' \in \mathcal{K}$ such that $R_{k^{(t+1,\phi(\bar{k})-1)}} \cap R_{k'} = \emptyset$,
 402 we have $|A_{\phi(\bar{k})-1} \cap R_{k'}| = 0 \leq \zeta'_{k'}$. Furthermore,

$$\begin{aligned} |A_{\phi(\bar{k})-1} \cap R_{k^{(t+1,\phi(\bar{k}))}}| &= |A_{\phi(\bar{k})} \cap R_{k^{(t+1,\phi(\bar{k}))}}| \\ &\leq \zeta_{k^{(t+1,\phi(\bar{k}))}} \end{aligned}$$

403 by construction of $A_{\phi(\bar{k})}$. Finally, for all k' such that $R_{k^{(t+1,\phi(\bar{k})-1)}} \subseteq R_{k'}$, $|A_{\phi(\bar{k})-1} \cap R_{k'}| = |A_{\phi(\bar{k})-1}| =$
 404 $V_{\mathfrak{R}}^*(S_t \cap R_{k^{(t+1,\phi(\bar{k})-1)}}) = |B|$ with the previously defined B , in particular $|B \cap R_{k'}| \leq \zeta_{k'}$, but given that
 405 $B \subseteq S_t \cap R_{k^{(t+1,\phi(\bar{k})-1)}}$, $|B \cap R_{k'}| = |B|$. Wrapping all those equalities, it comes that $|A_{\phi(\bar{k})-1} \cap R_{k'}| \leq \zeta_{k'}$. In
 406 the end, $|A_{\phi(\bar{k})-1} \cap R_{k'}| \leq \zeta_{k'}$ for all $k' \in \mathcal{K}$, so $A_{\phi(\bar{k})-1}$ realizes the maximum in (25) for $S_t \cap R_{k^{(t+1,\phi(\bar{k})-1)}}$.

407 By applying exactly the same method, we recursively construct a non-increasing sequence $A_{\phi(\bar{k})} \subseteq$
 408 $\dots \subseteq A_1$ such that for all $\ell \in \{1, \dots, \phi(\bar{k})\}$ and $k' \in \mathcal{K}$, $A_\ell \subseteq S_t \cap R_{k^{(t+1,\ell)}}$, $V_{\mathfrak{R}}^*(S_t \cap R_{k^{(t+1,\ell)}}) = |A_\ell|$, and
 409 $|A_\ell \cap R_{k'}| \leq \zeta_{k'}$. Furthermore for $\ell' > \ell$, $A_\ell \setminus A_{\ell'} \subseteq S_t \cap R_{k^{(t+1,\ell)}} \setminus S_t \cap R_{k^{(t+1,\ell')}}$. Also note that the fact
 410 that $i_{t+1} \notin \bigcup_{k \in \mathcal{K}_t^-} R_k$ implies that $\eta_{k^{(t+1,\ell)}}^t < \zeta_{k^{(t+1,\ell)}}$ for all $\ell \in \{1, \dots, \phi(\bar{k})\}$. So by (16), $|A_\ell| < \zeta_{k^{(t+1,\ell)}}$.

411 Let, for any $\ell \in \{1, \dots, \phi(\bar{k})\}$, $\tilde{A}_\ell = A_\ell \cup \{i_{t+1}\}$. Given that $A_\ell \subseteq S_t \cap R_{k^{(t+1,\ell)}}$ and that $i_{t+1} \in S_{t+1} \setminus S_t$,
 412 $\tilde{A}_\ell \subseteq S_{t+1} \cap R_{k^{(t+1,\ell)}}$, $|\tilde{A}_\ell| = |A_\ell| + 1$, and for all $\ell' \in \{1, \dots, \phi(\bar{k})\}$, $|\tilde{A}_\ell \cap R_{k^{(t+1,\ell')}}| = |A_\ell \cap R_{k^{(t+1,\ell')}}| + 1$.
 413 Note that if, furthermore, $\ell \geq \ell'$, then $A_\ell \subseteq A_{\ell'}$, so

$$\begin{aligned} |\tilde{A}_\ell \cap R_{k^{(t+1,\ell')}}| &= |A_\ell \cap R_{k^{(t+1,\ell')}}| + 1 \\ &\leq |A_{\ell'} \cap R_{k^{(t+1,\ell')}}| + 1 \\ &= |A_{\ell'}| + 1 \\ &< \zeta_{k^{(t+1,\ell')}} + 1. \end{aligned}$$

414 On the contrary, if $\ell < \ell'$, we write that

$$\begin{aligned} |\tilde{A}_\ell \cap R_{k^{(t+1,\ell')}}| &= |A_\ell \cap R_{k^{(t+1,\ell')}}| + 1 \\ &= |(A_\ell \setminus A_{\ell'}) \cap R_{k^{(t+1,\ell')}}| + |A_{\ell'} \cap R_{k^{(t+1,\ell')}}| + 1 \\ &< 0 + \zeta_{k^{(t+1,\ell')}} + 1, \end{aligned}$$

415 because $A_\ell \setminus A_{\ell'} \subseteq R_{k^{(t+1,\ell)}} \setminus R_{k^{(t+1,\ell')}}$ hence $(A_\ell \setminus A_{\ell'}) \cap R_{k^{(t+1,\ell')}} = \emptyset$. In both cases, $|\tilde{A}_\ell \cap R_{k^{(t+1,\ell')}}| <$
 416 $\zeta_{k^{(t+1,\ell')}} + 1$ so $|\tilde{A}_\ell \cap R_{k^{(t+1,\ell')}}| \leq \zeta_{k^{(t+1,\ell')}}$. Additionally, for all $k' \in \mathcal{K}$ such that $i_{t+1} \notin R_{k'}$, $|\tilde{A}_\ell \cap R_{k'}| =$
 417 $|A_\ell \cap R_{k'}| \leq \zeta_{k'}$.

418 In the end, $|\tilde{A}_\ell \cap R_{k'}| \leq \zeta_{k'}$ for all $k' \in \mathcal{K}$, so

$$\begin{aligned} V_{\mathfrak{R}}^*(S_{t+1} \cap R_{k^{(t+1,\ell)}}) &\geq |\tilde{A}_\ell| \text{ by (25)} \\ &= |A_\ell| + 1 \\ &= V_{\mathfrak{R}}^*(S_t \cap R_{k^{(t+1,\ell)}}) + 1. \end{aligned}$$

419 So, as we wanted, $V_{\mathfrak{R}}^*(S_{t+1} \cap R_k) \geq V_{\mathfrak{R}}^*(S_t \cap R_k) + 1$ for all $k \in \mathcal{K}_t$ such that $i_{t+1} \in R_k$ and so for all
420 such k that are in \mathcal{K}_{t+1} . So every inequality in (24) becomes an equality and we have proven that

$$V_{\mathfrak{R}}^*(S_{t+1} \cap R_k) = V_{\mathfrak{R}}^*(S_t \cap R_k) + 1 = \eta_k^t + 1 = \eta_k^{t+1},$$

421 that is, (16) is true at $t + 1$. Looking at the first line of (24), we also proved that

$$V_{\mathfrak{R}}^*(S_{t+1} \cap R_k) = \sum_{\substack{k' \in \mathcal{P}^t \\ R_{k'} \subseteq R_k}} \zeta_{k'} \wedge |S_{t+1} \cap R_{k'}|. \quad (26)$$

422 The only thing left to prove is that (26) is also true with \mathcal{P}^{t+1} instead of \mathcal{P}^t , that is that (17) also
423 holds at $t + 1$, or, put differently, that

$$\sum_{\substack{k' \in \mathcal{P}^t \\ R_{k'} \subseteq R_k}} \zeta_{k'} \wedge |S_{t+1} \cap R_{k'}| = \sum_{\substack{k' \in \mathcal{P}^{t+1} \\ R_{k'} \subseteq R_k}} \zeta_{k'} \wedge |S_{t+1} \cap R_{k'}|. \quad (27)$$

424 If h_{t+1}^f does not exist, meaning that we didn't break the loop, $\mathcal{P}^{t+1} = \mathcal{P}^t$ so there is nothing to prove.

425 Now assume that h_{t+1}^f exists. So (23) holds. We will split each term in (27) in a sum of two terms.

426 First, note that by (23), for any $k' \in \mathcal{K}$ such that $R_{k'} \cap R_{k^{(t+1, h_{t+1}^f)}} = \emptyset$, we have that $k' \in \mathcal{P}^{t+1}$ if and
427 only if $k' \in \mathcal{P}^t$. And so,

$$\begin{aligned} \sum_{\substack{k' \in \mathcal{P}^{t+1} \\ R_{k'} \subseteq R_k}} \zeta_{k'} \wedge |S_{t+1} \cap R_{k'}| &= \sum_{\substack{k' \in \mathcal{P}^{t+1} \\ R_{k'} \cap R_{k^{(t+1, h_{t+1}^f)}} = \emptyset \\ R_{k'} \subseteq R_k}} \zeta_{k'} \wedge |S_{t+1} \cap R_{k'}| + \zeta_{k^{(t+1, h_{t+1}^f)}} \wedge |S_{t+1} \cap R_{k^{(t+1, h_{t+1}^f)}}| \\ &= \sum_{\substack{k' \in \mathcal{P}^t \\ R_{k'} \cap R_{k^{(t+1, h_{t+1}^f)}} = \emptyset \\ R_{k'} \subseteq R_k}} \zeta_{k'} \wedge |S_{t+1} \cap R_{k'}| + \zeta_{k^{(t+1, h_{t+1}^f)}} \wedge |S_{t+1} \cap R_{k^{(t+1, h_{t+1}^f)}}|. \end{aligned}$$

428 Recall that we already proved that there is no $k' \in \mathcal{P}^t$ such that $R_{k^{(t+1, h_{t+1}^f)}} \subsetneq R_{k'}$, so for any $k' \in \mathcal{P}^t$,
429 either $R_{k'} \cap R_{k^{(t+1, h_{t+1}^f)}} = \emptyset$ or $R_{k'} \subseteq R_{k^{(t+1, h_{t+1}^f)}}$. Hence the split

$$\begin{aligned} \sum_{\substack{k' \in \mathcal{P}^t \\ R_{k'} \subseteq R_k}} \zeta_{k'} \wedge |S_{t+1} \cap R_{k'}| &= \sum_{\substack{k' \in \mathcal{P}^t \\ R_{k'} \cap R_{k^{(t+1, h_{t+1}^f)}} = \emptyset \\ R_{k'} \subseteq R_k}} \zeta_{k'} \wedge |S_{t+1} \cap R_{k'}| + \sum_{\substack{k' \in \mathcal{P}^t \\ R_{k'} \subseteq R_{k^{(t+1, h_{t+1}^f)}} \\ R_{k'} \subseteq R_k}} \zeta_{k'} \wedge |S_{t+1} \cap R_{k'}| \\ &= \sum_{\substack{k' \in \mathcal{P}^t \\ R_{k'} \cap R_{k^{(t+1, h_{t+1}^f)}} = \emptyset \\ R_{k'} \subseteq R_k}} \zeta_{k'} \wedge |S_{t+1} \cap R_{k'}| + \sum_{\substack{k' \in \mathcal{P}^t \\ R_{k'} \subseteq R_{k^{(t+1, h_{t+1}^f)}}}} \zeta_{k'} \wedge |S_{t+1} \cap R_{k'}|, \end{aligned}$$

430 where the last equality comes from the fact that $R_{k^{(t+1, h_{t+1}^f)}} \subseteq R_k$, because $k \in \mathcal{K}_{t+1}$, $i_{t+1} \in R_k$, and
431 $k^{(t+1, h_{t+1}^f)} \in \mathcal{P}^{t+1}$.

432 Given the two previously made splits, it remains to prove that

$$\sum_{\substack{k' \in \mathcal{P}^t \\ R_{k'} \subseteq R_{k^{(t+1, h_{t+1}^f)}}}} \zeta_{k'} \wedge |S_{t+1} \cap R_{k'}| = \zeta_{k^{(t+1, h_{t+1}^f)}} \wedge |S_{t+1} \cap R_{k^{(t+1, h_{t+1}^f)}}|.$$

433 Interestingly, this does not depend on k anymore. By (26), the left-hand side is equal to $V_{\mathfrak{R}}^*(S_{t+1} \cap$
 434 $R_{k^{(t+1, h_{t+1}^f)}})$. Because we are breaking the loop at step h_{t+1}^f , $\eta_{k^{(t+1, h_{t+1}^f)}}^{t+1} = \zeta_{k^{(t+1, h_{t+1}^f)}}$. Finally, because (16)
 435 holds at $t+1$, $\eta_{k^{(t+1, h_{t+1}^f)}}^{t+1} = V_{\mathfrak{R}}^*(S_{t+1} \cap R_{k^{(t+1, h_{t+1}^f)}})$. Wrapping all these assertions:

$$\begin{aligned} \sum_{\substack{k' \in \mathcal{P}^t \\ R_{k'} \subseteq R_{k^{(t+1, h_{t+1}^f)}}}} \zeta_{k'} \wedge |S_{t+1} \cap R_{k'}| &= V_{\mathfrak{R}}^*(S_{t+1} \cap R_{k^{(t+1, h_{t+1}^f)}}) \\ &= V_{\mathfrak{R}}^*(S_{t+1} \cap R_{k^{(t+1, h_{t+1}^f)}}) \wedge |S_{t+1} \cap R_{k^{(t+1, h_{t+1}^f)}}| \\ &= \eta_{k^{(t+1, h_{t+1}^f)}}^{t+1} \wedge |S_{t+1} \cap R_{k^{(t+1, h_{t+1}^f)}}| \\ &= \zeta_{k^{(t+1, h_{t+1}^f)}} \wedge |S_{t+1} \cap R_{k^{(t+1, h_{t+1}^f)}}|, \end{aligned}$$

436 which achieves the second case and so the proof. \square

437 4 Implementation

438 All algorithms discussed in this manuscript are already implemented in the R (R Core Team, 2024)
 439 package `sanssouci` (Neuvial et al., 2024) which is available on GitHub (see the References for the link)
 440 and is dedicated to the computation of confidence bounds for the number of false positives. It also
 441 hosts the implementation of the methods described in Blanchard et al. (2020) and Enjalbert-Courrech
 442 and Neuvial (2022). Algorithm 1 is implemented as the `V.star` function, Algorithm 2 is implemented
 443 as the `pruning` function, and Algorithm 4 is implemented as the `curve.V.star.forest.fast` function
 444 (whereas the `curve.V.star.forest.naive` function just repeatedly calls `V.star`). Note that the
 445 `pruning` function has a `delete.gaps` option that speeds up the computation even more by removing
 446 unnecessary gaps introduced in the data structure by the `pruning` operation, those gaps being due to
 447 the specific structure that is used to store the information of \mathcal{K} .

448 Speaking of the data structure, we briefly describe it, with an example. We represent $(R_k)_{k \in \mathcal{K}}$ by two
 449 lists, `C` and `leaf_list`. `leaf_list` is a list of vectors, where `leaf_list[[i]]` is the vector listing
 450 the hypotheses in the atom P_i . `C` is a list of lists. For $1 \leq h \leq H$, `C[[h]]` lists the regions at depth h ,
 451 using the index bounds of the atoms they are composed of. That is, the elements of the list `C[[h]]`
 452 are vectors of size two, and if there is k, i and j such that `C[[h]][[k]] = c(i, j)`, it means that
 453 $(i, j) \in \mathcal{K}$, or in other words that $P_{i:j}$ is one of the regions, and that $\phi((i, j)) = h$. We emphasize that
 454 the 1D structure of the hypotheses has to be respected by the user as the current implementation
 455 implicitly uses it: that is, P_1 has to contain the hypotheses labeled $1, 2, \dots, p$, P_2 has to contain the
 456 hypotheses labeled $p+1, \dots$, and so on. Also, the hypotheses have to be in non-decreasing order:
 457 `leaf_list[[1]]` has to be equal to `c(1, 2, 3, \dots, p)` and not, say, `c(2, 1, 3, \dots, p)`.

458 **Example 4.1** (Implementation of Example 2.3). For the reference family given in Example 2.2 and
 459 completed in Example 2.3, $H = 3$. For $h = 1$, we have `C[[1]][[1]] = c(1, 5)`, `C[[1]][[2]] = c(6,`
 460 `7)`, `C[[1]][[3]] = c(8, 8)`. For $h = 2$, we have `C[[2]][[1]] = c(1, 1)`, `C[[2]][[2]] = c(2,`
 461 `3)`, `C[[2]][[3]] = c(4, 5)`, `C[[2]][[4]] = c(6, 6)`, `C[[2]][[5]] = c(7, 7)`. For $h = 3$, we
 462 have `C[[3]][[1]] = c(2, 2)`, `C[[3]][[2]] = c(3, 3)`, `C[[3]][[3]] = c(4, 4)`, `C[[3]][[4]] =`
 463 `c(5, 5)`.

464 And then for the atoms, we have `leaf_list[[1]] = c(1, 2)`, `leaf_list[[2]] = c(3, 4)`,
 465 `leaf_list[[3]] = c(5, 6, 7, 8, 9, 10)`, `leaf_list[[4]] = c(11, 12, 13, 14, 15, 16)`,
 466 `leaf_list[[5]] = c(17, 18, 19, 20)`, `leaf_list[[6]] = 21`, `leaf_list[[7]] = 22` and finally
 467 `leaf_list[[8]] = c(23, 24, 25)`.

468 The functions `dyadic.from.leaf_list`, `dyadic.from.window.size`, and `dyadic.from.height` re-
 469 turn the appropriate data structure to represent a \mathcal{K} that can be described as a dyadic tree, based on
 470 some entry parameters that can be inferred from the names of the functions. The completion of a
 471 forest structure, mentioned in Section 2.3, is done by the `forest.completion` function. Finally, the
 472 ζ_k 's are computed as in Durand et al. (2020) by the `zetas.tree` function with `method=zeta.DKWM`.

473 5 Numerical experiments

474 In this Section, we present some numerical experiments aiming to demonstrate the impact of the
 475 pruning of Algorithm 2 (using the `delete.gaps` option mentioned in Section 4) and of the fast
 476 Algorithm 4, in terms of computation time, compared to the only previously available method to
 477 compute a curve of confidence bounds. As mentioned in Section 2.3 and Section 4, this naive method
 478 simply consisted in a `for` loop repeatedly applying Algorithm 1.

479 To compare the computation time, we use the R package `microbenchmark` version 1.5.0 (Mersmann,
 480 2024) with R version 4.4.0 (2024-04-24) and `sanssouci` version 0.13.0, on a MacBook Air M1 (2020)
 481 running macOS 15.1.1. The package `microbenchmark` allows to run code snippets a given number
 482 `n_repl` of times, and to compute summary statistics on the computation time. The script executing
 483 the computation can be found in the same repository as this manuscript.

484 Four scenarios are studied, all based on a common setting which we first describe. A number m of
 485 hypotheses is tested. We use a reference family (R_k, ζ_k) such that the R_k 's have a forest structure of
 486 maximal depth $H = 10$. The graph of the inclusion relations between the R_k 's is a binary tree, hence
 487 there are $2^H - 1 = 1023$ R_k 's and in particular $2^{H-1} = 512$ atoms. P -values are generated in a gaussian
 488 one-sided fashion where $H_{0,i} = \{\mathcal{N}(\mu, \text{Id}) : \mu_i = 0\}$, $H_{1,i} = \{\mathcal{N}(\mu, \text{Id}) : \mu_i = 4\}$, and $p_i(X) = 1 - \Phi(X_i)$.
 489 \mathcal{H}_1 is comprised of the leafs 1, 5, 9 and 10, that is $\mathcal{H}_1 = P_1 \cup P_5 \cup P_9 \cup P_{10}$. For each scenario, the
 490 curve $(V_{\mathfrak{R}}^*(\{1, \dots, t\}))_{t \in \mathbb{N}_m^*}$ is computed. For the experiments including pruning, the pruning is done
 491 once before the `n_repl` replications, to mimick the practice where pruning only needs to be done
 492 once and for all, while the user may be interested in computing multiple bounds and curves after
 493 that.

494 In scenarios 1 and 2, $m = 1024$ (so the atoms are of size 2), in scenarios 3 and 4, $m = 10240$ (so the
 495 atoms are of size 10). In scenarios 1 and 3, the ζ_k 's are estimated trivially by $\zeta_k = |R_k|$, and in scenarios
 496 2 and 4, they are computed as in Durand et al. (2020) with the DKWM inequality (Dvoretzky et al.,
 497 1956, ; Massart, 1990). Because of the size of m and the poor performances of the naive approach,
 498 we set `n_repl=100` in scenarios 1 and 2 and `n_repl=10` only in scenarios 3 and 4. The differences
 499 between the scenarios are summarized in Table 1.

Table 1: Differences between the scenarios

parameter	Scenario 1	Scenario 2	Scenario 3	Scenario 4
m	1024	1024	10240	10240
zeta computation	trivial	DKWM	trivial	DKWM
<code>n_repl</code>	100	100	10	10

500 For the trivial ζ_k computation of scenarios 1 and 3, the pruning obviously deletes all non-atom regions
 501 so $|\mathcal{K}^{\text{pr}}| = 512$. Whereas, for the particular instance $\omega \in \Omega$ in the experiments, $|\mathcal{K}^{\text{pr}}| = 541$ for
 502 scenario 2, and $|\mathcal{K}^{\text{pr}}| = 573$ for scenario 4. Those results alone illustrate the benefits of pruning with
 503 respect to the reduction of the cardinality of the reference family: the regions above atoms with no
 504 signal (or no detectable signal in the trivial scenarios) are pruned. The fact that the regions above

505 atoms with detectable signal are not pruned means that they are relevant for the confidences bounds
 506 (which had already been demonstrated in the simulation study of [Durand et al. \(2020\)](#)).

507 The summary statistics of the computation time in each scenario are presented in Table 2, Table 3,
 508 Table 4, and Table 5, and they are also presented as boxplots in Figure 11. The time unit is the second
 509 (in logarithmic scale in the boxplots).

Table 2: Scenario 1

expr	min	lq	mean	median	uq	max	neval
naive.not.pruned	3.6924007	3.7943906	3.8521256	3.8386487	3.8780412	4.5247099	100
naive.pruned	3.2822354	3.4126177	3.4758338	3.4614076	3.5061541	3.8822089	100
fast.not.pruned	0.1332744	0.1367000	0.1383806	0.1385039	0.1392707	0.1768691	100
fast.pruned	0.0921422	0.0945472	0.0974025	0.0954231	0.0978687	0.1908498	100

Table 3: Scenario 2

expr	min	lq	mean	median	uq	max	neval
naive.not.pruned	3.7280744	3.8025695	3.8514710	3.8451367	3.8831009	4.1891831	100
naive.pruned	3.3556131	3.4533210	3.4926114	3.4906796	3.5182172	3.8501820	100
fast.not.pruned	0.1214844	0.1246071	0.1265674	0.1260760	0.1279640	0.1407320	100
fast.pruned	0.0815349	0.0827995	0.0841622	0.0835618	0.0851062	0.0896013	100

Table 4: Scenario 3

expr	min	lq	mean	median	uq	max	neval
naive.not.pruned	332.1856576	335.5148922	337.9856658	338.2432916	340.3329972	344.6255264	10
naive.pruned	328.3186707	329.3081834	332.1861199	331.4335773	333.3563651	338.7111614	10
fast.not.pruned	1.4881838	1.4966417	1.5066370	1.5078498	1.5151194	1.5217546	10
fast.pruned	0.9354581	0.9418174	0.9498806	0.9512573	0.9550453	0.9675895	10

Table 5: Scenario 4

expr	min	lq	mean	median	uq	max	neval
naive.not.pruned	331.0124665	335.6357519	349.7740812	337.6459728	342.1652204	401.4881647	10
naive.pruned	331.2567637	332.2215437	363.5822362	333.0651271	335.8347696	493.5124771	10
fast.not.pruned	1.3575818	1.3588461	1.3733567	1.3641336	1.3762178	1.4460291	10
fast.pruned	0.9287399	0.9441687	0.9551275	0.9520622	0.9624959	0.9972532	10

510 On each scenario, using the fast algorithm is much faster than the naive approach, while pruning
 511 always gives a slight improvement over not pruning.

512 Comparing scenarios 1 and 2 first, we see that, as expected, there is no significant change in
 513 computation time for `naive.not.pruned`, while `naive.pruned` is faster in scenario 1, given that we
 514 prune more. But, on the other hand, `fast.not.pruned` and `fast.pruned` are both faster in scenario
 515 2, even if we prune less. This is because, for the regions with signal, said signal is detected and so

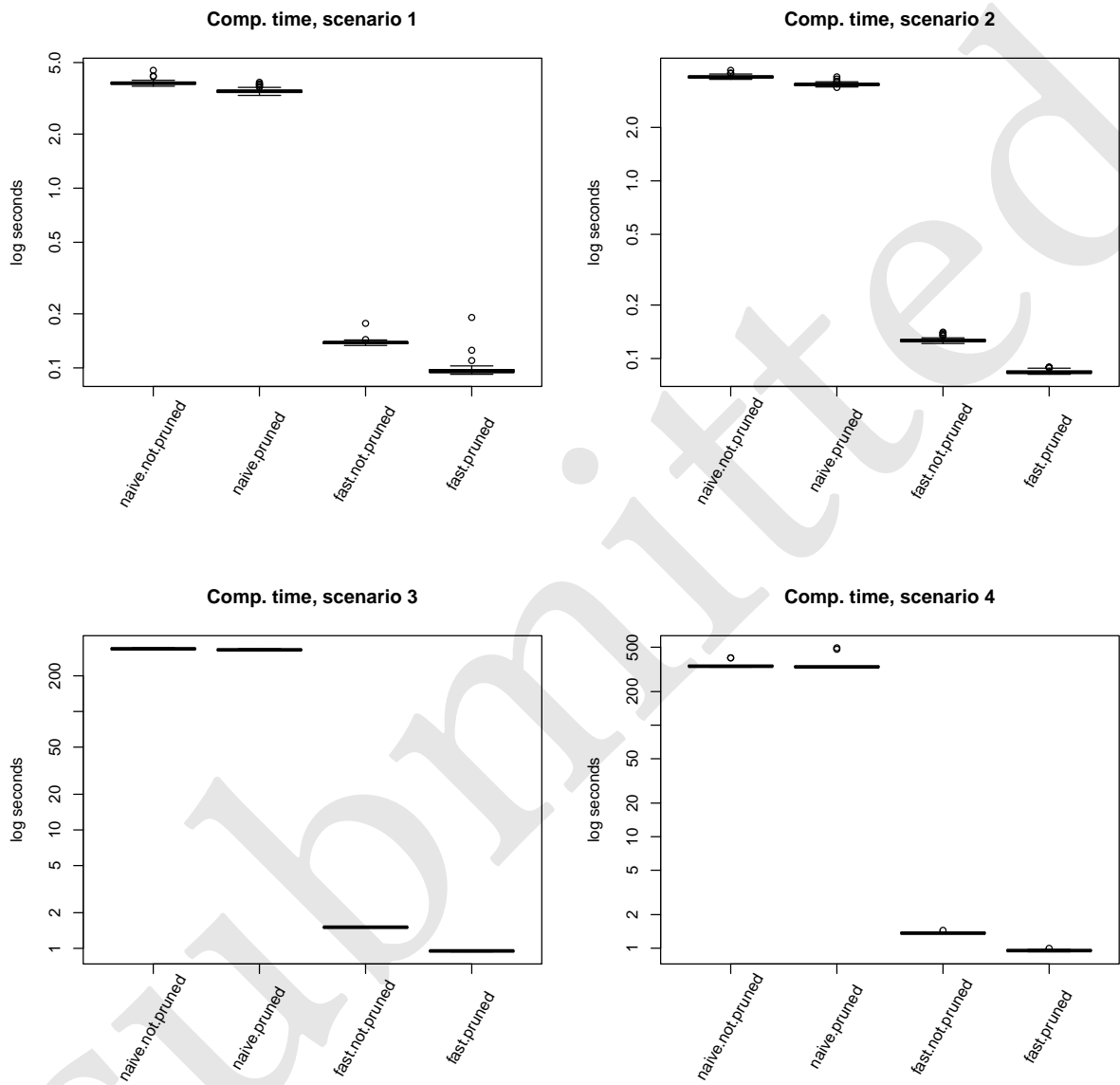


Figure 11: Computation times in scenario, in log seconds

516 those regions are quickly saturated, in the sense that we quickly have $\eta_k^t = \zeta_k$ and k added to \mathcal{K}_k^- ,
517 which saves a lot of time.

518 The comparison between scenarios 3 and 4 is similar, except that this time we prune even less in
519 scenario 4 and so the effect of the saturation is not enough to compensate. Although, with only
520 `n_repl=10`, the statistics seem less accurate, this can be confirmed with additional experiments
521 (`n_repl` can also be set to 100 without problem if we don't include `naive` methods).

522 Finally, comparing scenarios 3 & 4 with scenarios 1 & 2, we see that multiplying the number of
523 hypotheses by 10 effectively multiplies the computation time by ~ 10 when using Algorithm 4 and
524 by ~ 100 when using Algorithm 1 naively, which illustrates the stated complexities of $O(m|\mathcal{K}|)$ and
525 $O(m^2|\mathcal{K}|)$, respectively.

526 6 Conclusion

527 In conclusion, we effectively introduced a new algorithm to compute a curve of confidence upper
528 bounds, much faster than the previous alternative, with one power of m less in the complexity.

529 To develop new confidence upper bounds methodology and test them on simulations, it was previously
530 not conceivable to replicate experiments a sufficient number of times while computing whole curves.
531 For instance, in the simulation study of Durand et al. (2020), the number of replications chosen was
532 10 and the whole curve was not computed, only ten values along the curve were computed, for an
533 `m` set to 12800, that is 0.078% of the curve had been computed. Now, simulation studies with an
534 adequate number of replications and 100% of the curve become feasible.

535 A lot of work remains to be done on the `sanssouci` package. For example, to make the data format of
536 a forest structure $(R_k)_{k \in \mathcal{K}}$ less convoluted and more user-friendly is an interesting project. Another
537 one would be to implement inside the package the methods of the paper Blain et al. (2022), which
538 are currently only available in the Python language (Van Rossum and Drake, 2009), and the methods
539 of the paper Meah et al. (2024).

540 Other current works include the development of new reference families with theoretical JER control
541 that could better account for realistic models, such as models with dependence between the p -values,
542 see for example Perrot-Dockès et al. (2023), or models with discreteness.

543 7 Acknowledgements

544 This work has been supported by ANR-20-IDEES-0002 (PIA), ANR-19-CHIA-0021 (BISCOTTE), ANR-
545 23-CE40-0018 (BACKUP) and ANR-21-CE23-0035 (ASCAI). Thanks to Romain Périer for being the
546 first to extensively use the new implemented algorithms.

547 References

- 548 Yoav Benjamini and Yosef Hochberg. Controlling the false discovery rate: a practical and powerful
549 approach to multiple testing. *J. Roy. Statist. Soc. Ser. B*, 57(1):289–300, 1995. ISSN 0035-9246. URL
550 <https://www.jstor.org/stable/2346101>.
- 551 Alexandre Blain, Bertrand Thirion, and Pierre Neuvial. Notip: Non-parametric True Discovery
552 Proportion control for brain imaging. *Neuroimage*, 260, October 2022. URL <https://doi.org/10.1016/j.neuroimage.2022.119492>.

- 554 Gilles Blanchard, Pierre Neuvial, and Etienne Roquain. Post hoc confidence bounds on false positives
555 using reference families. *Ann. Statist.*, 48(3):1281–1303, 2020. ISSN 0090-5364. doi: 10.1214/19-
556 AOS1847. URL <https://doi.org/10.1214/19-AOS1847>.
- 557 Małgorzata Bogdan, Ewout van den Berg, Chiara Sabatti, Weijie Su, and Emmanuel J. Candès. SLOPE—
558 adaptive variable selection via convex optimization. *Ann. Appl. Stat.*, 9(3):1103–1140, 2015. ISSN
559 1932-6157,1941-7330. doi: 10.1214/15-AOAS842. URL <https://doi.org/10.1214/15-AOAS842>.
- 560 Guillermo Durand, Gilles Blanchard, Pierre Neuvial, and Etienne Roquain. Post hoc false positive
561 control for structured hypotheses. *Scand. J. Stat.*, 47(4):1114–1148, 2020. ISSN 0303-6898. doi:
562 10.1111/sjos.12453. URL <https://doi.org/10.1111/sjos.12453>.
- 563 A. Dvoretzky, J. Kiefer, and J. Wolfowitz. Asymptotic minimax character of the sample distribution
564 function and of the classical multinomial estimator. *Ann. Math. Statist.*, 27:642–669, 1956. ISSN
565 0003-4851. doi: 10.1214/aoms/1177728174. URL <https://doi.org/10.1214/aoms/1177728174>.
- 566 Nicolas Enjalbert-Courrech and Pierre Neuvial. Powerful and interpretable control of false discoveries
567 in two-group differential expression studies. *Bioinformatics*, 38(23):5214–5221, 10 2022. ISSN 1367-
568 4803. doi: 10.1093/bioinformatics/btac693. URL <https://doi.org/10.1093/bioinformatics/btac693>.
- 569 Christopher R. Genovese and Larry Wasserman. Exceedance control of the false discovery proportion.
570 *J. Amer. Statist. Assoc.*, 101(476):1408–1417, 2006. ISSN 0162-1459. doi: 10.1198/016214506000000339.
571 URL <https://doi.org/10.1198/016214506000000339>.
- 572 Jelle J. Goeman and Aldo Solari. Multiple testing for exploratory research. *Statist. Sci.*, 26(4):584–597,
573 2011. ISSN 0883-4237. doi: 10.1214/11-STS356. URL <https://doi.org/10.1214/11-STS356>.
- 574 Ruth Marcus, Eric Peritz, and K. R. Gabriel. On closed testing procedures with special reference
575 to ordered analysis of variance. *Biometrika*, 63(3):655–660, 1976. ISSN 0006-3444. doi: 10.1093/
576 biomet/63.3.655. URL <https://doi.org/10.1093/biomet/63.3.655>.
- 577 P. Massart. The tight constant in the Dvoretzky-Kiefer-Wolfowitz inequality. *Ann. Probab.*, 18(3):
578 1269–1283, 1990. ISSN 0091-1798,2168-894X. URL [http://links.jstor.org/sici?doi=0091-1798\(199007\)18:3<1269:TTCITD>2.0.CO;2-Q&origin=MSN](http://links.jstor.org/sici?doi=0091-1798(199007)18:3<1269:TTCITD>2.0.CO;2-Q&origin=MSN).
- 580 Iqraa Meah, Gilles Blanchard, and Etienne Roquain. False discovery proportion envelopes with
581 m-consistency. *Journal of Machine Learning Research*, 25(270):1–52, 2024. URL <http://jmlr.org/papers/v25/23-1025.html>.
- 583 Rosa J. Meijer, Thijmen J. P. Krebs, and Jelle J. Goeman. A region-based multiple testing method for
584 hypotheses ordered in space or time. *Stat. Appl. Genet. Mol. Biol.*, 14(1):1–19, 2015. ISSN 2194-6302.
585 doi: 10.1515/sagmb-2013-0075. URL <https://doi.org/10.1515/sagmb-2013-0075>.
- 586 Nicolai Meinshausen. False discovery control for multiple tests of association under general depen-
587 dence. *Scand. J. Statist.*, 33(2):227–237, 2006. ISSN 0303-6898. doi: 10.1111/j.1467-9469.2005.00488.x.
588 URL <https://doi.org/10.1111/j.1467-9469.2005.00488.x>.
- 589 Olaf Mersmann. *microbenchmark: Accurate Timing Functions*, 2024. URL <https://CRAN.R-project.org/package=microbenchmark>. R package version 1.5.0.
- 591 Pierre Neuvial, Gilles Blanchard, Guillermo Durand, Nicolas Enjalbert-Courrech, and Etienne Roquain.
592 *sanssouci: Post Hoc Multiple Testing Inference*, 2024. URL <https://sanssouci-org.github.io/sanssouci>.
593 R package version 0.13.0.
- 594 Marie Perrot-Dockès, Gilles Blanchard, Pierre Neuvial, and Etienne Roquain. Selective inference for
595 false discovery proportion in a hidden markov model. *TEST*, pages 1–27, 2023.

596 R Core Team. *R: A Language and Environment for Statistical Computing*. R Foundation for Statistical
597 Computing, Vienna, Austria, 2024. URL <https://www.R-project.org/>.
598 Guido Van Rossum and Fred L. Drake. *Python 3 Reference Manual*. CreateSpace, Scotts Valley, CA,
599 2009. ISBN 1441412697.
600 Anna Vesely, Livio Finos, and Jelle J. Goeman. Permutation-based true discovery guarantee by sum
601 tests. *J. R. Stat. Soc. Ser. B. Stat. Methodol.*, 85(3):664–683, 2023. ISSN 1369-7412,1467-9868. doi:
602 10.1093/jrsssb/qkad019. URL <https://doi.org/10.1093/jrsssb/qkad019>.

603 Session information

604 R version 4.4.0 (2024-04-24)
605 Platform: aarch64-apple-darwin21.6.0
606 Running under: macOS 15.1.1
607
608 Matrix products: default
609 BLAS: /opt/homebrew/Cellar/openblas/0.3.29/lib/libopenblas-r0.3.29.dylib
610 LAPACK: /opt/homebrew/Cellar/r/4.4.0_1/lib/R/lib/libRlapack.dylib; LAPACK version 3.12.0
611
612 locale:
613 [1] en_US.UTF-8/en_US.UTF-8/en_US.UTF-8/C/en_US.UTF-8/en_US.UTF-8
614
615 time zone: Europe/Paris
616 tzcode source: internal
617
618 attached base packages:
619 [1] stats graphics grDevices datasets utils methods base
620
621 other attached packages:
622 [1] microbenchmark_1.5.0
623
624 loaded via a namespace (and not attached):
625 [1] compiler_4.4.0 fastmap_1.1.1 cli_3.6.2 htmltools_0.5.8.1
626 [5] tools_4.4.0 yaml_2.3.8 tinytex_0.51 rmarkdown_2.26
627 [9] knitr_1.46 jsonlite_1.8.8 xfun_0.43 digest_0.6.35
628 [13] rlang_1.1.3 renv_1.0.7 evaluate_0.23